

Universidade do Minho
Escola de Ciências

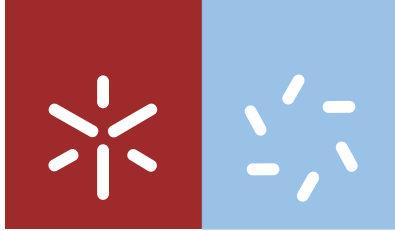
André Eduardo Carneiro Dias

**Versatile route to approach nanoscale
protein multiplexing**

André Eduardo Carneiro Dias Versatile route to approach nanoscale protein multiplexing

UMinho | 2013

outubro de 2013



Universidade do Minho
Escola de Ciências

André Eduardo Carneiro Dias

Versatile route to approach nanoscale protein multiplexing

Dissertação de Mestrado
Mestrado em Biofísica e Bionanossistemas

Trabalho realizado sob a orientação da
Doutora Karen L. Martinez
e do
Prof. Doutor Paulo José Gomes Coutinho

DECLARAÇÃO

Nome: André Eduardo Carneiro Dias

Endereço eletrónico: andreecdias@gmail.com

Número do Bilhete de Identidade: 13506658

Título da dissertação:

Versatile route to approach nanoscale protein multiplexing

Orientador:

Doutora Karen L. Martinez

Prof. Doutor Paulo José Gomes Coutinho

Ano de conclusão: 2013

É AUTORIZADA A REPRODUÇÃO INTEGRAL DESTA DISSERTAÇÃO APENAS PARA EFEITOS DE INVESTIGAÇÃO, MEDIANTE DECLARAÇÃO ESCRITA DO INTERESSADO, QUE A TAL SE COMPROMETE

Universidade do Minho, ___/ ___/ _____

Assinatura: _____

Acknowledgements

First of all, I would like to thank my parents, without whom I would never have the chance to embark on this adventure that has been my master degree and my stay in Denmark.

I would like to thank my supervisor, Dr. Karen L. Martinez from the University of Copenhagen for giving me the chance to work in her research group and for all the pieces of advice that have contributed for the completion of this thesis.

For all the help and scientific knowledge provided during this research project, I would like to thank Eduardo Della Pia. Thanks for the patience, all the pieces of advice, all the time spent teaching me and, most of all, for being a great friend.

To everyone in the research group for the good moments spent together and for all the support given me, thank you. It was a great pleasure knowing and working with all of you.

I would also like to thank my co-supervisor, Dr. Paulo Coutinho, for his availability whenever I needed.

To all my friends, thank you for helping me stay true to myself and for all the relaxation moments.

Finally, I would like to thank the International Relations Office for granting me the Erasmus scholarship that allowed me to do the research work leading to this thesis in the Nano-Science Center of the University of Copenhagen.

Abstract

On the last decade protein arrays have earned a highlight place in drug discovery or to study protein-protein interaction. The miniaturization of such systems and the ability to study interactions with several proteins at the same time has been proven invaluable in these fields.

More recently, with the inclusion of protein arrays in microfluidic devices, these platforms have also been used in biosensing or bioanalytics. However, despite the fundamental breakthroughs that have been made in the development of such devices, there still is a need to develop new strategies which allow the reduction of the amount of protein used, the reduction of the area on which the proteins are immobilized and the immobilization of multiple proteins using soft conditions.

This thesis reports two different approaches to immobilize proteins: by coordination of polyhistidine-tag to Ni-NTA motifs on the surface of polystyrene microparticles and by directing proteins onto the surface of a conductive polymer, polypyrrole, by applying an electric field.

H₆-EGFP and SNAP-Flag-His₁₀ were expressed in *E. coli* and purified using immobilized metal affinity chromatography and size exclusion chromatography.

The binding of H₆-EGFP onto polystyrene microparticles covered with Ni-NTA motifs is analyzed by fluorescence spectroscopy and fluorescence microscopy. It is also shown how immobilization of functionalized particles can be used for the creation of inexpensive protein microarrays.

The second approach described shows how the sequential electrogeneration of polypyrrole films can be used to immobilize different proteins on distinct electrodes of a single array. It is also shown how the use of an electric field may enhance the adsorption of the proteins onto the polypyrrole film.

Sumário

Na última década, arrays de proteínas ganharam um lugar de destaque na descoberta de fármacos ou no estudo de interações proteína-proteína. A miniaturização destes sistemas e a capacidade de estudar interações com várias proteínas ao mesmo tempo provou ser importantíssimo nestas áreas.

Mais recentemente, com a aplicação de arrays de proteínas em dispositivos microfluidicos, estas plataformas também foram usadas como biosensores ou em bioanalítica. No entanto, e apesar dos avanços fundamentais no desenvolvimento de tais dispositivos, ainda existe a necessidade de desenvolver novas estratégias que permitam reduzir a quantidade de proteína usada, reduzir a área sobre a qual as proteínas são imobilizadas e a imobilização de várias proteínas usando condições suaves.

Esta tese relata duas estratégias de imobilização de proteínas diferentes: por coordenação de sequências de poli-histidina com motivos Ni-NTA na superfície de micropartículas de poliestireno e por direcionamento de proteínas para a superfície de um polímero condutor, polipirrole, por aplicação de um campo eléctrico.

H₆-EGFP e SNAP-Flag-His₁₀ foram expressas em E. Coli e purificadas por cromatografia de afinidade com metal imobilizado e cromatografia por exclusão de tamanho.

A adsorção de H₆-EGFP à superfície de micropartículas de poliestireno cobertas com motivos Ni-NTA é analisada por espectroscopia de fluorescência e por microscopia de fluorescência. Também se mostra como a imobilização de partículas funcionalizadas pode ser usada para a criação de microarrays de proteínas economicamente acessíveis.

A segunda estratégia descrita mostra a como electrogeração sequencial de filmes de polipirrole pode ser usada para imobilizar diferentes proteínas em eletrodos distintos dum único array. É também mostrado como o uso de um campo eléctrico pode aumentar a adsorção de proteínas à superfície do filme de polipirrole.

Table of contents

Chapter 1. Introduction	page	1
1.1. Protein arrays	page	3
1.2. Fabrication methods.	page	4
1.3. Surface modification	page	5
1.4. Outline	page	7
Chapter 2. Molecular Biology	page	9
2.1. Introduction	page	11
2.1.1. Aim of the project	page	11
2.1.2. Enhanced Green Fluorescent Protein	page	11
2.1.3. SNAP-tag	page	13
2.2. Material and Methods	page	14
2.2.1. H ₆ -EGFP expression	page	14
2.2.2. H ₆ -EGFP purification	page	14
2.2.3. SFH ₁₀ expression	page	15
2.2.4. SFH ₁₀ purification	page	15
2.2.5. Labelling of the SNAP-Tag	page	16
2.2.6. Cleavage of the His-tag	page	16
2.2.7. BCA assays	page	17
2.2.8. SDS-PAGE gels	page	17
2.2.9. Fluorescence spectra	page	17
2.3. Results and Discussion	page	19
2.3.1. Expression and purification of H ₆ -EGFP	page	19
2.3.2. Expression, purification and labelling of SFH ₁₀	page	22
2.3.3. Cleavage of the his-tag from SFH ₁₀	page	24
2.4. Conclusion	page	27

Chapter 3. Analysis of protein binding on polystyrene microparticles	page	29
3.1. Introduction	page	31
3.1.1. Aim of the project	page	31
3.1.2. Polystyrene microspheres	page	31
3.1.3. Nitriloacetate complexes	page	32
3.2. Materials and methods	page	34
3.2.1. Functionalization of polystyrene microparticles in solution	page	34
3.2.2. Immobilization of polystyrene microparticles on a glass surface	page	34
3.2.3. Absorbance spectra	page	35
3.2.4. Fluorescence spectra	page	35
3.2.5. Fluorescence microscopy	page	35
3.3. Results and discussion	page	36
3.3.1. Analysis of polystyrene microscopy by fluorescence spectroscopy	page	36
3.3.2. Analysis of polystyrene microparticles by fluorescence microscopy	page	39
3.3.3. Immobilization of functionalized polystyrene microparticles on a glass surface.....	page	44
3.4. Conclusion	page	46
 Chapter 4. Directed protein immobilization: approaching nanoscale protein multiplexing	page	47
4.1. Introduction	page	49
4.1.1. Aim of the project	page	49
4.1.2. Conducting polymers	page	49
4.1.3. Ion migration within an electric field	page	50
4.2. Materials and methods	page	52
4.2.1. Microelectrode arrays	page	52
4.2.2. Assembly of the electrochemical cell	page	52
4.2.3. Electropolymerization of the polypyrrole film	page	53

4.2.4. Functionalization of the electrodes	page	53
4.2.5. Fluorescence Microscopy	page	53
4.3. Results and discussion	page	54
4.4. Conclusion	page	62
Chapter 5. Summary and Perspectives.....	page	63
References	page	67
Annexes	page	73

Abbreviations

AFM.....	atomic force microscope
BG	O ⁶ -benzylguanine
DNA	deoxyribonucleic acid
DOL.....	degree of labeling
DPN	dip-pen nanolithography
EDTA.....	ethylenediaminetetraacetate
EGFP.....	enhanced green fluorescent protein
FPLC	fast performance liquid chromatography
GFP	green fluorescent protein
H ₆ -EGFP.....	EGFP containing an hexahistidine tag on its N-Terminus
hAGT	Human O ⁶ -alkylguanine-DNA alkyltransferase
IMAC	immobilized metal affinity chromatography
IPTG	Isopropyl β-D-1-thiogalactopyranoside
Ni-NTA.....	nickel nitriloacetate
NiNTA-PPsMPs	polystyrene microparticles covered with Ni-NTA.
NTA	nitriloacetate
OD _x	absorbance at "x" nm
PBS	phosphate buffer saline
PMSF	phenylmethanesulfonylfluoride
PPy	polypyrrole
SEC	size exclusion chromatography
SFH ₁₀	SNAP-Flag-His ₁₀
SPR.....	Surface Plasmon Resonance
SFH ₁₀ -647.....	SFH10 labeled with SNAP-Surface [®] 647
wtGFP	wild type GFP

Chapter 1.

Introduction

This master thesis deals with the immobilization of proteins on surfaces. Proteins are major biological components, being involved in many regulatory processes. While many approaches have been used to study these molecules, current techniques for protein immobilization are time consuming and require a lot of effort and material. It is important to develop new approaches to solve these problems.

Micro-/nanotechnology have provided an alternative. By immobilizing proteins on surfaces, we can more easily detect any changes occurring on the protein^[1-2]. Especially when miniaturizing the surface area covered by proteins, any changes to the existing protein layer may translate in a big change in the system's properties.

Here, I describe two different approaches that can be used to immobilize proteins on surfaces. The first one revolves around the use of a histidine-tag (his-tag) to immobilize proteins on polystyrene microspheres and the analysis of this system.

The second approach reports the sequential generation and functionalization of a polymer film, a polypyrrole (PPy) film, to immobilize different proteins on different micro-/nanoelectrodes of a single array. Additionally, it is also reported the use of an electric field to enhance protein adsorption on the polymer film.

1.1. Protein arrays

In the last few years, protein microarrays have had a deep impact on protein assays. These setups have allowed a high throughput parallel screening of biomarkers, protein-protein and protein-drug interactions, being used primarily in areas as drug discovery or diagnostics^[1, 3-6].

Nonetheless the dissemination of protein arrays has not been as expressive as deoxyribonucleic acid (DNA) arrays. Unlike DNA, proteins are very sensitive and chemical treatment of the surface often results in protein denaturation^[1,7]. In fact, the complexity of the fabrication of protein arrays has hindered their introduction in the marketplace.

More recently, biotechnological fields as bioanalytics, biocatalysis or biosensors have acted as a driving force for the development of protein biochips. Most protein microarrays use fluorescence detection due to the availability of fluorophores as well as the wide range of properties assessable, however label-free techniques, such as surface plasmon resonance or bioelectroanalytical techniques, have been rising as an alternative^[1,8,9].

Miniaturization has also played an important role on the development of protein biochips. The transition from microarrays to nanoarrays allows the reduction of materials required, being more cost effective and at the same time increasing the

number of measurements that can be performed with on a single chip and, thus, the statistical significance of the parameters determined^[1,2]. Moreover, in principle, at such small features, the binding of a single molecule to the surface is translated into a large variation of the surface's properties, improving the sensitivity of the assay and its detection limit.

Many techniques have been developed to allow highly controllable nanopatterning of proteins, however very few reports have shown multiple proteins patterned on nanoarrays so far. One other setback of protein arrays in contrast with DNA arrays is the background signal^[2,7]. DNA has a net negative charge, due the phosphate bridges linking the constitutive nucleotide, and its interaction with surfaces is promoted primarily by electrostatic interactions of these groups. By coating the surface with a negatively charged layer, it is possible to prevent the adsorption of DNA due to the electrostatic repulsion between the two. Proteins have both positive and negatively charged domains, hydrophobic and hydrophilic pockets and, as their interaction with surfaces is controlled by different forces, more complex strategies are required to decrease the background signal.

1.2. Fabrication methods

Most fabrication methods have been thoroughly described in many excellent reviews^[2,10,11]. The aim of this chapter is to give a short overview of the characteristics of different fabrication methods while providing some insight in the most prominent techniques.

Most reports of protein micro-/nanoarrays use techniques such as microcontact printing, soft lithography or UV lithography. These techniques allow to pattern surfaces with nanometer sized features in a fast and highly reproducible manner through the use of a mask^[2,7,11]. Electron beam lithography also has a prominent place in nanofabrication as it allows a resolution as low as 2 nm when patterning inorganic resists^[12]. Nonetheless, the fabrication method is very slow, being used mostly in order to produce masks to be applied on other techniques. A major setback of these techniques is that the whole surface must be covered with solution, allowing proteins to be immobilized on all the patterned regions.

Dip-Pen Nanolithography (DPN) and its variations have allowed multiple proteins to be patterned on the same array while maintaining up to a 40 nm resolution^[13-15]. DPN relies on an Atomic Force Microscope (AFM) tip forming a water meniscus on the surface and allowing the protein to be deposited. The molecule deposition time is directly dependent on the molecule size and the surface area to be functionalized,

meaning that the sequential immobilization of large proteins or patterning of large areas may take a lot of time. To circumvent the low throughput of the technique, cantilever arrays have been used in order to pattern proteins in a highly parallel manner. Despite DPN showing great promise in the patterning of small molecules, there are other factors which must be considered when patterning proteins. First, the protein “ink” used to functionalize the surface usually contains a carrier or a surfactant. This surfactant is used to prevent protein adsorption to the AFM tip and to increase the transfer speed of the molecule to the surface, however it might also result in reducing the adsorption to the surface. Also, if successive immobilization steps are performed, the conditions required may lead to the loss of conformation and, thus, to a loss of function.

1.3. Surface modification

The chemical and physical properties of the surface influence specific and non-specific binding of the proteins to the surface. It is, therefore, of vital importance to tune these properties in order to optimize the performance of a protein array.

Protein adsorption can be classified according to the covalent character of the bond and the proteins orientation (figure 1)^[7].

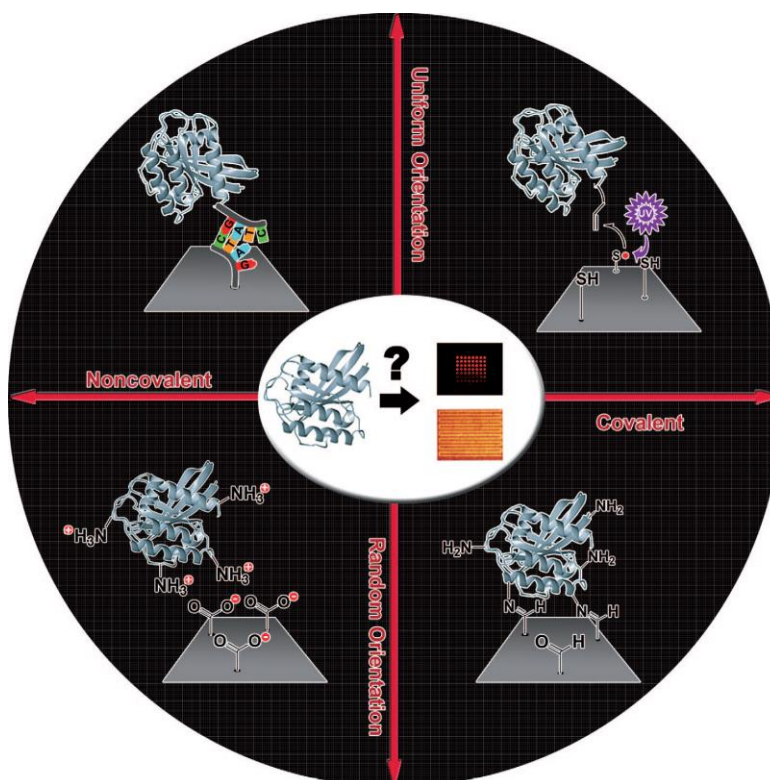


Figure 1. Schematic representation of the classification of protein adsorption strategies. Adapted from [7].

As mentioned above, proteins interact with a surface by ionic bonds, Van Der Waals forces and electrostatic, hydrophobic or polar interactions. Which intermolecular force dominates the interaction depends on the protein and surface involved. Random physisorption still represents one of the most common immobilization strategies, especially when functionalizing 3D surfaces (micro/nanoparticles, nanotubes, nanowires, etc). Amine- or carboxyl-modified surfaces are usually used with this strategy^[7]. The resulting protein layer is usually heterogeneous and randomly oriented.

Another strategy relying on non-covalent bonds is by using a polymer layer trapping the protein inside its matrix. Hydrogels on gold constitute the most common polymer surface used as they are usually used in Biacore or other similar technologies using surface plasmon resonance (SPR) measurements^[16,17].

Gold surfaces can also be functionalized with thiol- or amine-containing molecules by simply exploiting the high affinity of these residues for the gold surfaces. However when in direct contact with the gold, proteins tend to lose their conformation and, therefore, their function^[7]. To circumvent this problem, SAMs can be used as an intermediate layer, distancing the protein from the gold surface and even providing the surface with different characteristics.

Amine and carboxyl reactive groups can be used to form covalent bonds. Depending on the coupling reagents these groups target different functional groups^[7,18]. As we can usually find amine or carboxyl groups over the proteins' surface, the resulting protein layer tends to have a random orientation.

By immobilizing proteins with a certain orientation, in principle, we can facilitate interactions with other molecules. Current methods to immobilize proteins with a specific orientation were originally designed for fusion protein purification and adapted to protein arrays. By using a tag on fusion proteins to attach to the surface, one can create a uniformly oriented protein layer^[7,19].

Oligonucleotide tagged proteins use the DNA base pairing to specifically bind to the complementary oligonucleotides immobilized on the surface. This strategy shows a high stability and uses the established DNA arrays fabrication methods^[7]. One other alternative commonly used is the biotin-tag. Biotin can specifically bind to avidin, streptavidin or neutravidin. Even though this interaction does not result from a covalent bond, the high affinity between both molecules makes this bond nearly irreversible^[7,20]. Nickel Nitriloacetate (Ni-NTA) arrays use transition metal chemistry in order to bind histidine (his) tagged proteins^[7,21]. This system offers the possibility to elute bound proteins by addition of ethylenediaminetetraacetate (EDTA) or imidazole. The Ni-NTA complex will be reviewed in further detail in chapter 3.

So far, only strategies to bind proteins to a surface have been mentioned. However, it is also important to prevent the unwanted protein immobilization as this may result in high background signal. This can be achieved by selecting the surface used. Naturally occurring surfaces as elastin, agarose, cellulose or polysaccharides or, more commonly, synthetic polymers as polyethyleneglycol have been shown to prevent protein adsorption to their surface. Alternatively bovine serum albumin (BSA) or milk can be used to block the surface preventing further adsorption from other molecules. The use of surfactants as Tween 20 or sodium dodecyl sulfate (SDS) may also suppress non-specific protein adsorption ^[7].

1.4. Outline

The work described in this thesis was performed in Karen L. Martinez's group, at the Bionano and Nanomedicine laboratory of the University of Copenhagen. During my stay in the group, I had the opportunity to work in an international and multidisciplinary environment which, ultimately, has led to the development of this thesis.

Throughout this thesis many different concepts are introduced and they are organized in such a way that allows the reader to understand the scientific importance of the work described.

This short introduction chapter aims at giving a brief overview of the scientific landscape common to the different approaches described in the remaining chapters.

The second chapter of this thesis includes all the experiments within the molecular biology field. The chapter reports the expression and purification of two different proteins that would be used at later stages (chapters 3 and 4). This chapter also reports the characterization of the samples using spectroscopic techniques.

In chapter 3, the immobilization of his-tagged proteins on the surface of polystyrene microspheres (or microparticles) is reported. The particles were analyzed by fluorescence spectroscopy and later by fluorescence microscopy.

The fourth chapter reports the generation of a polypyrrole film on a micro-/nanoelectrode array as a platform to immobilize protein. It is shown how, by sequentially generating different films, one can immobilize different proteins on the same array. This chapter also investigates how the use of electric fields are a promising strategy to enhance protein adsorption. Such a strategy can be used to optimize conditions so it is possible to reduce the amount of protein required.

The final chapter summarizes the results and conclusions obtained in this thesis. Additionally, a perspective on future possibilities and future work required is also included in the chapter.

Chapter 2.

Molecular Biology

2.1. Introduction

2.1.1. Aim of the project

The first part of the project involved the expression and purification of model proteins to be used in later experiments (described in chapters 2 and 3). The proteins were selected to satisfy specific criteria related on how they would be used. The proteins are soluble in aqueous solution in order to simplify their handling, they possess fluorescent properties to allow an easy detection by fluorescence spectroscopy or fluorescence microscopy and, as a Ni-NTA motif was used in some of the experiments, the proteins also contain a His-tag either on the N-terminus or the C-terminus.

The first protein selected was an enhanced green fluorescent protein (EGFP) containing an hexahistidine-tag on its N-terminus (H₆-EGFP)(the aminoacid sequence for the protein can be found in annex). This protein respects the previously described properties and some of its other characteristics make it an ideal tool to use as a model protein. The most important of these is the fact that fluorescence emission is dependent on the interaction between the chromophore in its center and the correctly folded EGFP scaffold. Upon fluorescence microscopy analysis, this property allows us to easily assess whether or not the protein retains its structure.

The second model protein selected was the SNAP-Flag-His₁₀ (SFH₁₀). This model protein is formed by three different tags which have independent properties: the SNAP-tag (in the N-terminus), the Flag-tag and a decahistidine-tag (in the C-terminus). Even though, by itself, this protein is not fluorescent, it can be easily labelled using the SNAP-tag and its versatility allows it to be used in several different ways^[22]. First of all, the SNAP-tag substrate can be selected according to the requirements of the systems. The Flag-tag can be used to bind to an antibody and the His-tag allows the protein to easily bind to Ni-NTA motifs.

2.1.2. Enhanced Green Fluorescent Protein

Green Fluorescent Protein (GFP) from the jellyfish *Aequorea victoria* was first discovered by Osamu Shimonura^[23,24]. This 26.9 kDa protein emits green fluorescence upon excitation with blue or ultraviolet light, property that has attracted a lot of attention to its use as a biomarker since it was first expressed in living cells^[25,26] and its fluorescent properties have been improved^[27,28].

While the wild type GFP (wtGFP) shows low emission upon excitation with blue light (figure 2), the work developed by Tsien *et al*^[28], followed by Cormack *et al*^[29] has led to the creation of a double mutant protein carrying the mutation Ser65→Thr and Phe64→Leu, the EGFP. Comparing to the wtGFP, this mutant is more stable and shows a 5-fold increase upon excitation with blue light.

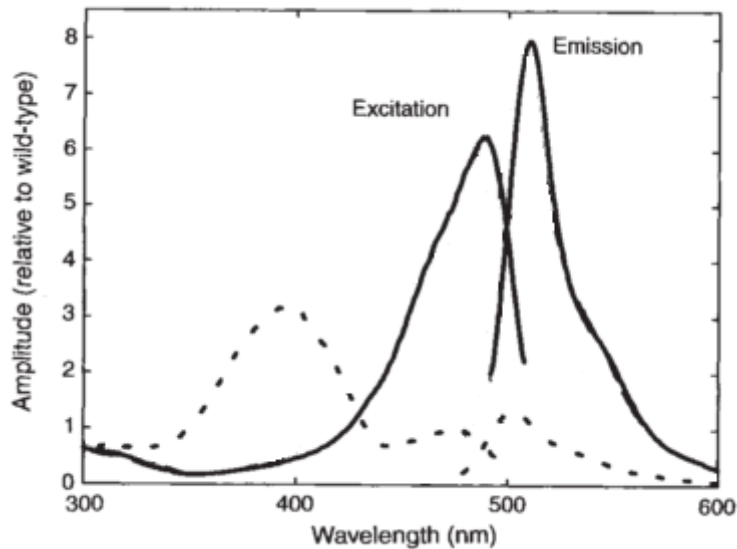


Figure 2. Excitation and emission spectra of wtGFP (- - -) and the Ser65→Thr mutant (—). Adapted from Tsien *et al*.

EGFP is an 11-stranded- β -barrel encapsulating a helix which runs up the central axis and upon which the chromophore is inserted^[30]. The chromophore (a *p*-hydroxybenzylideneimidazidone) is, thus, protected from the solvent and rigidified to turn fluorescent (in case the protein is denatured the chromophore shows no fluorescence).

Looking at the absorbance spectrum, the protein shows 3 major absorbance peaks in the UV-vis region: two peaks at 400 nm and 488 nm related with the protonated and deprotonated forms of the chromophore and one peak at 280 nm corresponding to the absorption of the aromatic aminoacids. A further decomposition of the visible region of the spectrum by fitting to Gaussians functions has shown three peaks at 400 nm , 470 nm and 490 nm. The last two correspond to two transitions to different excited states of the deprotonated form of the chromophore^[31].

2.1.3. SNAP-Tag

While fluorescent proteins can be used to study dynamic processes, protein-protein interactions and even conformational changes, their application is limited by the array of proteins available. Recently, there has been a request for a more versatile approach. An alternative is the selective labeling of fusion proteins.

Human O⁶-alkylguanine-DNA alkyltransferase (hAGT) has the function of repairing O⁶-alkylated guanines by transferring this alkyl group to a cysteine residue in its aminoacid chain (figure 3, A). O⁶-benzylguanine (BG) can also react with hAGT, property which enables its use as an inhibitor for this protein^[22,31]. Johnson *et al*^[31] have also shown that BG derivatives can be reacted with hAGT using the same mechanism (figure 3, B). Further optimization of the protein has led to an increase of the hAGT activity and disruption of its interaction with DNA^[33]. Furthermore, using this mutant hAGT, Johnson *et al*^[33] have also shown some of its potential as a biomarker.

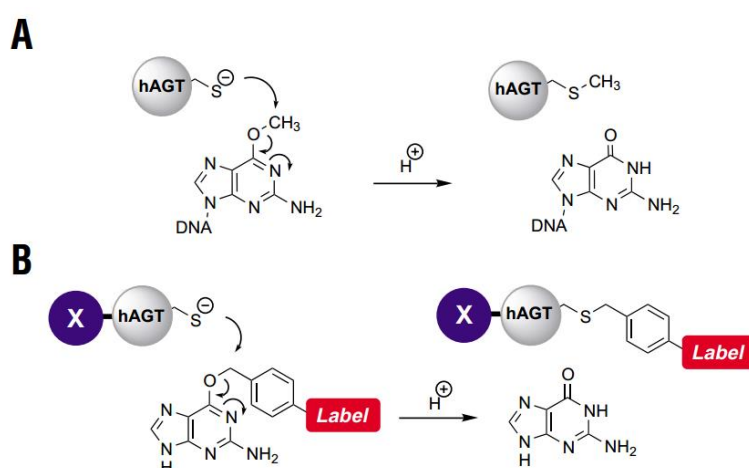


Figure 3. (A) DNA repair mechanism by hAGT. (B) Labeling mechanism of a X-hAGT fusion protein using a BG derivative. Adapted from [31].

A mutant hAGT is commercialized by New England BioLabs[®] Inc. named as SNAP-tag, which can be used to label SNAP-tag fusion proteins. The company also provides a set of BG derivatives, such as SNAP-Vista[®] Green, a BG labeled with fluorescein, or SNAP-Surface[®] 647, based on Dynamics Dye DY-647. Alternatively, BG derivatives can also be reacted with any molecule of interest in order to provide the BG derivative with the intended properties.

2.2. Materials and methods

2.2.1. H₆-EGFP expression

Expression of H₆-EGFP (Addgene) was carried out using *E. coli*, BL21 (DE3). The bacteria cells transformed with pUCBB-eGFP were inoculated in 20 mL Luria-Bertani (LB) medium containing 100 µg mL⁻¹ ampicillin and kept at 37 °C and 250 rpm, overnight. A new culture was then prepared with absorbance at 600 nm (OD₆₀₀) of 0.1 (OD₆₀₀ was measured using an Eppendorf® BioPhotometer) and grown at 37 °C and 250 rpm. Protein expression was induced by adding Isopropyl β-D-1-thiogalactopyranoside (IPTG) up to a final concentration of 0.1 mM at absorbance at 600 nm (OD₆₀₀) of 0.8. After inducing expression, the cells were grown at 37°C and 250 rpm for 2 hours. At this point, the bacteria cells were harvested by centrifuging at 2 000 g for 30 min using Eppendorf® centrifuge 5810 R. The pellet was kept frozen at -20°C until further use.

In order to lyse the cells, they were resuspended in phosphate buffer saline (PBS) (0.138 M NaCl, 0.0027 M KCl, pH 7.4) (Sigma). Then, phenylmethanesulfonyl fluoride (PMSF) and Lysozyme were added to a final concentration of 1 mM and 1 mg mL⁻¹, respectively. The cells were then incubated for 30 min, on ice and in the dark and anti-protease cocktail (Thermo Scientific) was added to the solution. The lysate was sonicated for 2 min (10 s bursts with 10 s cooling between). The soluble fraction was then recovered by centrifuging at 14 000g, 4 °C for 45 min (Eppendorf® centrifuge 5810 R).

2.2.2. H₆-EGFP purification

H₆-EGFP was purified from the supernatant by immobilized metal affinity chromatography (IMAC). For this, a HisTrap column (GE Healthcare) was used on a fast performance liquid chromatography (FPLC) system (Äkta purifier, Amersham Biosciences). The protein was inserted into the column and unwanted proteins were washed away using binding buffer (20 mM sodium phosphate, 500 mM NaCl, 20 mM imidazole, pH=7.4). The remaining protein was eluted with elution buffer (20 mM sodium phosphate, 500 mM NaCl, 500 mM imidazole, pH=7.4).

The first time the protein was expressed a HiTrap column (GE Healthcare) on a FPLC system was used to desalt the solution. To further purify the protein of interest, a size exclusion chromatography (SEC) was performed using a Superdex 200 10/300 GL (GE Healthcare) column in association with the FPLC system (Äkta purifier, Amersham

Biosciences) and using PBS as medium. The optimized purification protocol (used on the second time I expressed the protein) uses a SEC to purify the protein immediately after purification through IMAC with PBS as medium.

2.2.3. SFH₁₀ expression

To express SFH₁₀, previously cloned *E. coli* BL21 was streaked out on a LB agar plate and kept overnight at 37 °C. It was then inoculated in 15 mL LB containing 150 µg mL⁻¹ ampicillin and incubated overnight, at 37 °C, 240 rpm.

A new culture was then prepared with starting OD₆₀₀ of 0.1 in 1.5 L LB containing 150 µg mL⁻¹ ampicillin, 5 µM ZnCl₂ and kept at 37 °C. Upon measuring an OD₆₀₀ of 0.8, expression was induced by adding IPTG up to a final concentration of 0.5 mM and the culture was incubated at 30 °C, 240 rpm for 4 h.

The cells were harvested by centrifuging at 2 000 g for 30 min (Eppendorf® centrifuge 5810 R). They were then stored at -20 °C until required.

To lyse the cells, they were resuspended in 50 mM sodium phosphate, 500mM NaCl, 20 mM imidazole, pH 7.4 and PMSF and lysozyme were added to a final concentration of 1mM and 1 mg mL⁻¹, respectively. The mixture was kept on ice for 30 min and anti-protease cocktail (Thermo Scientific) was added.

The lysate was sonicated for 2 min (10 s bursts with 10 s cooling between) and centrifuged at 14 000g for 45 min. at 4°C (Eppendorf® centrifuge 5810 R) in order to pellet the cellular debris. The supernatant was recovered and kept at -20°C overnight.

2.2.4. SFH₁₀ purification

SFH₁₀ was purified from the supernatant of the lysate by gradient IMAC. For this, the protein was inserted into the HisTrap column using the FPLC system (Äkta purifier, Amersham Biosciences) and, immediately after, the gradient was started using only sodium phosphate buffer (20 mM sodium phosphate, 500 mM NaCl, pH 7.4) and increasing the concentration of elution buffer .

After purification through IMAC, the a HiTrap column (GE Healthcare) on the FPLC system was used to exchange the buffer to PBS. For this, the sample was inserted into the column and eluted by using PBS as medium.

2.2.5. Labelling of the SNAP-Tag

The SNAP-Tag from SFH₁₀ was labeled by mixing SFH₁₀ and SNAP-Tag substrate (either SNAP-Vista[®] Green or SNAP-Surface[®] 647, from New England BioLabs, previously dissolved in DMSO) with a 1:2 ratio (fusion protein : substrate) in 50 mM Tris-HCl, 100 mM NaCl, 0.1% Tween 20, 5 mM DTT, pH 7.5. The mixture was kept in the dark, at room temperature, for 60 min. The excess SNAP-Tag substrate was removed using a Bio-Spin[®] P-30 gel column. Before using the column, it was washed four times with PBS in order to exchange the stock buffer. After removal of the unbound SNAP-Tag substrate, the sample was frozen at -20 °C until required.

The degree of labeling (DOL) corresponds to the ratio between the amount of fluorophore and fusion protein. This parameter was assessed according to:

$$DOL = \frac{OD_{647} \times \epsilon_{SFH}^{280}}{OD_{280} \times \epsilon_{BG647}^{647} - OD_{647} \times \epsilon_{BG647}^{280}}$$

where OD₆₄₇ and OD₂₈₀ are the absorbance of the labeled proteins at 647 nm and 280 nm, respectively. ϵ_{SFH}^{280} is the molar extinction coefficient of SFH₁₀ at 280 nm (22585 M⁻¹ cm⁻¹). ϵ_{BG647}^{280} and ϵ_{BG647}^{647} are the molar extinction coefficient of SNAP-Surface[®] 647 at 280 nm and 647 nm, respectively. Absorbance measurements were recorded in a 96-well UV-transparent microplate (Corning) using a Synergy H4 microplate reader (BioTek Instruments).

For SDS-PAGE analysis, the samples were labeled with SNAP-Vista[®] Green and run on a SDS-PAGE gel immediately after the labeling reaction. To detect the labeled protein in the SDS-PAGE gels a Dark Reader DR89X Transilluminator (Clare Chemical Research) was used before staining.

2.2.6. Cleavage of the His-tag

The His-tag was cleaved from SFH₁₀ by using EKMax[™] from Life Technologies[™].

Pilot reactions were set up by mixing different concentrations of EKMax[™] with 20 µg SFH₁₀ in 50 mM Tris-HCl, 1 mM CaCl₂, 0.1% Tween 20 (EKMax[™] Reaction Buffer) and incubating in the dark, at 37°C, overnight. The samples were then labeled with SNAP-Vista[®] Green and run on a SDS-Page gel.

After optimization, EKMax[™] was added to SFH₁₀ labeled with SNAP-Surface[®] 647 (SFH₁₀-647) (with a 20 µg SFH-647: 0.1 U EKMax[™] ratio) in EKMax[™] Reaction Buffer. The mixture was incubated in the dark, at 37 °C, overnight.

To isolate the different components, a SEC was performed using a Superdex 75 (GE Healthcare) column on a FPLC system. PBS was used as a medium and only the fractions correspondent to the protein of interest were kept. After separation, DTT was added to 1 mM to stabilize the protein.

2.2.7. BCA assays

To determine protein concentration, bicinchoninic acid (BCA) assays were performed using a Thermo Scientific Pierce BCA Protein Assay Kit according to the manufacturer's protocol.

Different concentrations of BSA as well as the samples were allowed to react with the provided reagents in a 96-well UV-transparent microplate (Corning) for 30 min at 37 °C. Absorbance at 562 nm was read on a Synergy H4 microplate reader (BioTek Instruments).

2.2.8. SDS-PAGE gels

For sodium dodecyl sulfate - polyacrylamide gel electrophoresis (SDS-PAGE) analysis NuPAGE[®] Bis-Tris precast gels from Life Technologies[™] were used.

The samples were prepared by mixing protein sample on a ratio of 6.5:10 (volume of protein : final volume), 4x NuPAGE[®] LDS Sample Buffer with a ratio 1:4 (NuPAGE[®] LDS Sample Buffer : final volume), 0.1 M DTT. The samples were then heated at 70°C for at least 15 min and loaded onto the gel.

The gels were run at 150 V for 50 min using NuPAGE[®] MES SDS Running Buffer as medium. Afterwards, the gels were stained with SimplyBlue[™] SafeStain (Life Technologies[™]) using the manufacturer's microwave procedure. They were imaged and analyzed using ImageJ.

2.2.9. Fluorescence spectra

Excitation and emission spectra of H₆-EGFP samples were measured on a Spex FluoroMax-4 spectrofluorometer (HORIBA, Jobin Yvon).

For the emission spectra, samples were excited at 400 nm (slit 3 nm) and emission spectra were monitored between 500 nm and 700 nm (slit 3 nm), with integration time of 0.5 s nm⁻¹ and with an increment of 1 nm. As for the excitation spectra, emission was monitored at 530 nm (slit 3nm) and excitation spectra were monitored between 260

and 510 nm (slit 3 nm), with integration time of 0.5 s nm⁻¹ and with an increment of 1 nm.

2.3. Results and Discussion

2.3.1. Expression and purification of H₆-EGFP

After lysing the bacteria cells and recovering the soluble fraction, the protein needs to be purified. As H₆-EGFP contains a His-tag, it can be easily purified by IMAC. By washing the column with buffer containing 20 mM imidazole, any protein without any affinity for the Ni-NTA motifs is washed away and ideally the only protein remaining would be H₆-EGFP. Then, it is possible to elute the protein by washing the column 500 mM imidazole (figure 4).

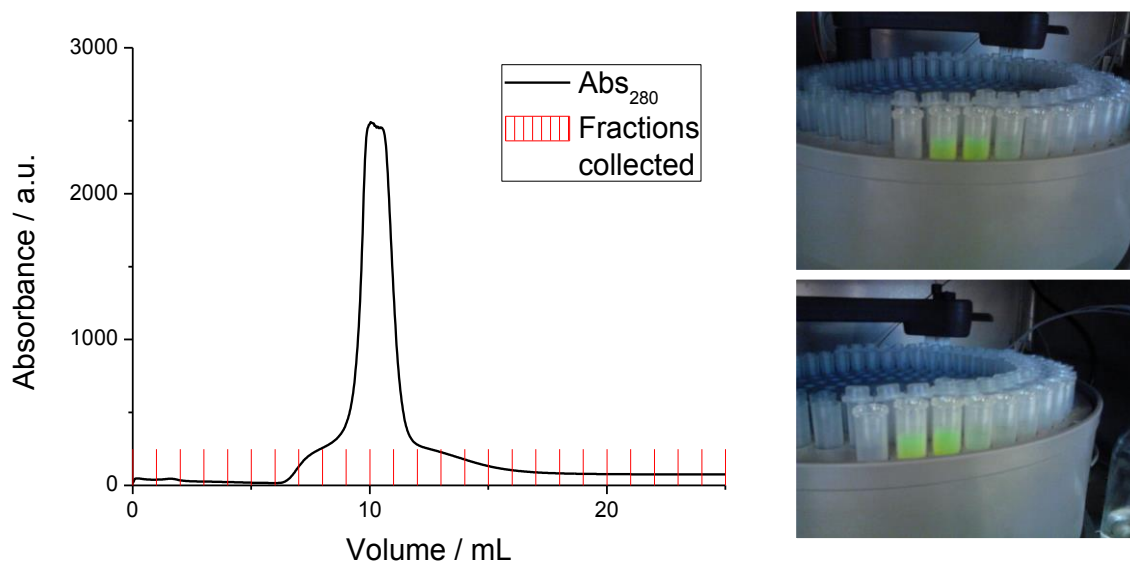


Figure 4. Chromatogram of the H₆-EGFP elution using IMAC (left) and images of the collected fractions (right).

The first time I used this protocol, absorbance was monitored only at 280 nm. This wavelength is where aromatic aminoacids absorb light at, so it is usually used to detect any protein. In the case of H₆-EGFP, however, besides monitoring only this wavelength, it should also be monitored absorbance at 488 nm, as this corresponds to the absorbance peak of the protein.

As the only information available from the chromatogram corresponds to the total protein concentration, it is expectable for the H₆-EGFP to correspond to the elution peak at 10 mL. This assumption was complemented by a visual control. As the protein emits green light, only the fractions which have a green color contain the protein (figure 4, right).

After elution, the protein is in presence of a high concentration of imidazole, which can be removed simply by exchanging the buffer. The proteins were characterized by

SDS-PAGE (figure 5) and ImageJ analysis at this point shows protein purity of 68.7 %. The presence of two extra bands after the desalting step can be explained by an upconcentration of the sample during this stage.

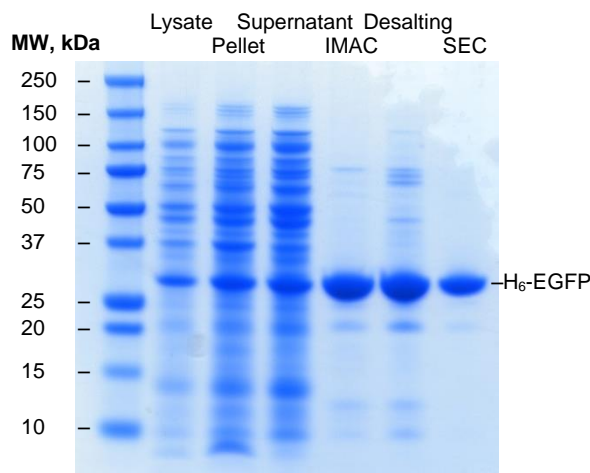


Figure 5. SDS-Page gel of the different stages of the first H₆-EGFP purification (indicated on the top of the gel).

Due to the impurities present in solution, the protein sample was further purified by SEC. During this stage absorbance was monitored at 280 nm and 488 nm (figure 6), corresponding the absorption peak of aromatic aminoacids and EGFP, respectively. Furthermore as the protein is approximately 28 kDa, it is expected to elute at 15 mL.

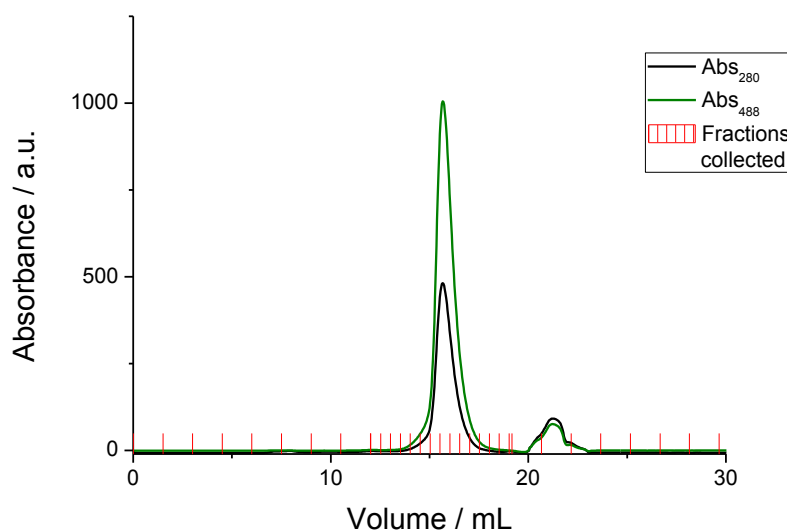


Figure 6. Chromatogram of the purification of the protein sample by SEC.

The SDS-Page analysis of the recovered protein (figure 6) shows that both the low- and high molecular weight impurities have been removed from the sample and its purity is 94.4 % as evaluated by ImageJ.

The sample was further characterized by fluorescence spectroscopy. Both the excitation and emission spectrum recorded (figure 8) match those found in the literature (figure 2) indicating the protein retains its functionality upon expression and purification

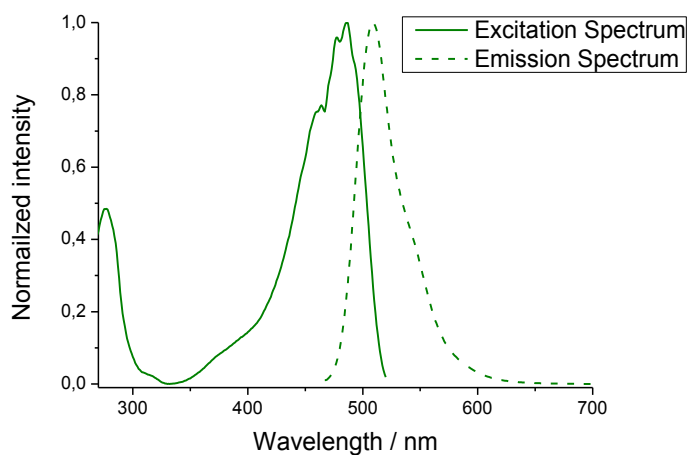


Figure 7. Excitation ($\lambda_{em}=530$ nm) and emission spectra ($\lambda_{ex}=400$ nm) of the protein sample after purification through IMAC and desalting.

The concentration of H₆-EGFP was determined by BCA assay indicating a yield of 1110 $\mu\text{g mL}^{-1}$ ($\approx 38 \mu\text{M}$).

After optimizing the purification protocol, the protein was expressed and purified a second time. The conditions used were the same as before, but there was no need to desalt the sample following the IMAC as the buffer exchange can also be done during the SEC (chromatograms shown in annex). As expected, the SDS-PAGE analysis from the second batch of protein (figure 8) shows that the contents of the purified protein sample are similar to the contents from the first batch. Total protein concentration as determined by BCA assay is 1625 $\mu\text{g mL}^{-1}$ ($\approx 56 \mu\text{M}$)

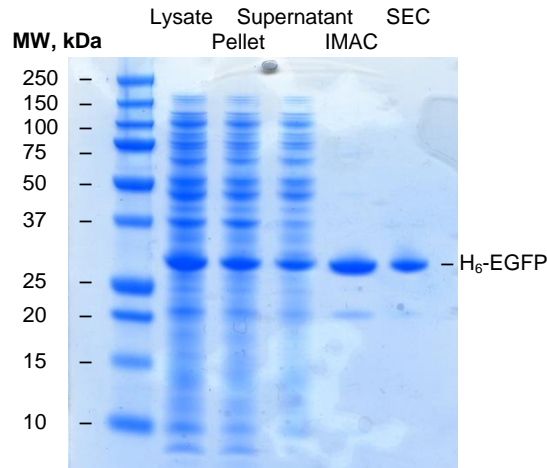


Figure 8. SDS-Page gel of the H₆-EGFP sample throughout the different steps taken on the 2nd purification.

2.3.2. Expression, Purification and labelling of SFH₁₀

Expression of SFH₁₀ on *E. coli* BL21 had previously been optimized in the lab, thus, the same conditions were used. Nonetheless, the IMAC purification protocol available had not been optimized for use in a FPLC yet. Preliminary experiments showed the presence of unwanted proteins with a high affinity for Ni-NTA. In order to isolate the proteins according to their affinity for these sites a gradient IMAC was performed. By monitoring absorbance at 280 nm (figure 9), three elution peaks are visible. An elution peak starting at 0 % elution buffer (0 mM imidazole), a second elution peak starting at ~38 % elution buffer (~190 mM imidazole) and a third peak starting at ~50 % elution buffer (250 mM imidazole).

The different fractions were labeled with SNAP-Vista[®] Green and characterized by SDS-PAGE (figure 10). By labeling the SNAP-Tag prior to SDS-PAGE analysis, it is possible to easily identify SNAP-fusion proteins upon excitation with blue light (figure 10, right), showing SFH₁₀ is present only in the third elution peak.

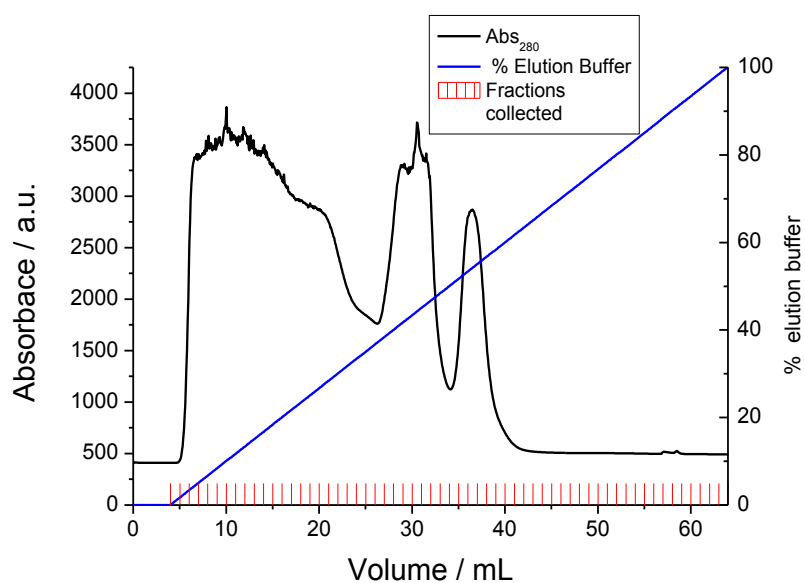


Figure 9. Chromatogram of the purification of SFH₁₀ using a gradient IMAC. %elution buffer corresponds to fraction of elution buffer used. At 0 % elution buffer there is no imidazole in the system while 100 % elution buffer corresponds to 500 mM imidazole.

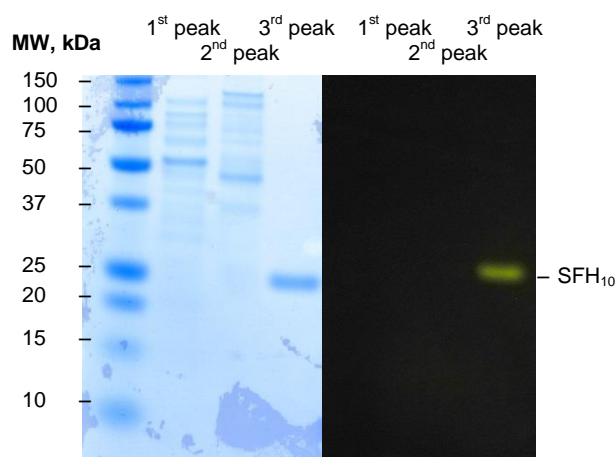


Figure 10. (Left) SDS-Page gel of samples from the different peaks in the gradient IMAC (figure 12). The samples were reacted with SNAP-Vista[®] Green prior to being run on the gel. (Right) Image of the same gel before staining and excited with blue light.

SDS-PAGE analysis of the protein sample throughout the purification procedure (figure 11) shows that all impurities have been removed from solution.

The concentration of SFH₁₀ was determined by BCA assay indicating a yield of 2671 $\mu\text{g mL}^{-1}$ ($\approx 118 \mu\text{M}$)

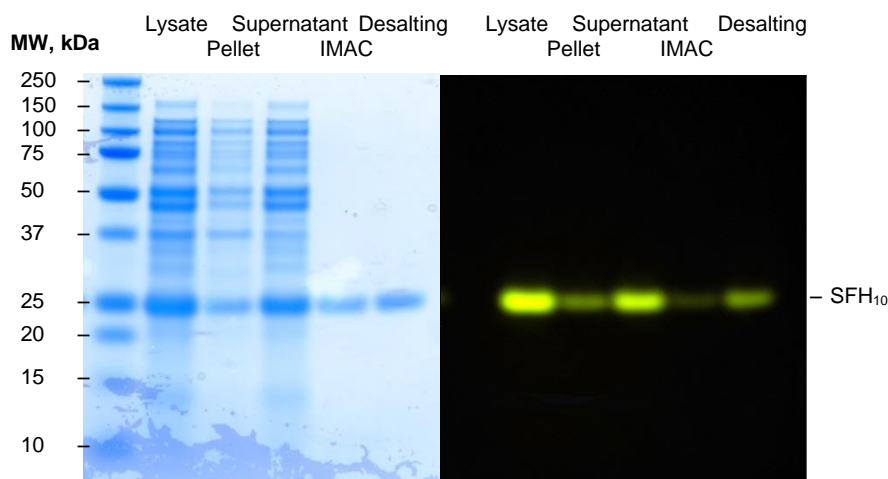


Figure 11. (Left) SDS-Page gel of SFH₁₀ samples throughout the purification (figure 12). The samples were reacted with SNAP-Vista[®] Green prior to being run on the gel. (Right) Image of the same gel before staining and excited with blue light.

Before using the protein in further experiments, the SNAP-tag was labeled with SNAP-Surface[®] 647. To characterize the labeling efficiency, the DOL was determined. Briefly, this parameter is the quotient of the concentration of fluorophore versus the concentration of protein. These elements were determined by measuring the absorbance of the labeled protein at 280 nm and 647 nm indicating a DOL of 64.58% (protein concentration = 15.5 μ M). The DOL is dependent on two major factors. First, it is inversely correlated to the protein purity. As protein concentration is determined by the absorbance at 280 nm, non-reactive proteins will also account for the determined DOL. Second, the DOL is directly correlated to the enzymatic activity of the SNAP-Tag fusion protein as a higher DOL means the SNAP-tag fusion protein was able to process more substrate during the reaction time. The DOL is specific for a set reaction as the substrate, temperature, pH, among other factors have an influence on the enzymatic activity.

2.3.3. Cleavage of the his-tag from SFH₁₀

The his-tag was also cleaved in order to assess its influence on the protein adsorption to a PPy film (experiment described in chapter 4). It is not known whether or not the his-tag influences DOL of the protein/cleaved protein, so in order to ensure this value is identical in both versions of the protein, the his-tag was cleaved after the protein was labelled. The cleavage of the his-tag is possible as the tag is located on the C-terminus, immediately following the Flag-tag. The Flag-tag has a cleavage site for Enterokinase on its C-terminus, which is usually used for cleaving this N-terminal tag

from fusion proteins. Nonetheless, the construct of SFH₁₀ allows this cleavage site to remove not the Flag-tag but the His-tag on its C-terminus.

As an insufficient amount of enzyme does not fully cleave the protein and an excessive amount might show unspecific cleavage, the first step in the process was to optimize the ratio protein: enzyme to be used. This was done by reacting SFH₁₀ with EKMax™, followed by labeling with SNAP-Vista® Green and finally analyzing on a SDS-Page gel (Figure 12).

As one would expect we see a small shift to smaller sizes when EKMax™ has been added to the solution due to the cleavage of the His-tag. The gel also shows that the optimal concentration is 20 µg SFH₁₀ per 0.1 U EKMax™, as ImageJ analysis of the protein band is clearer than for other concentrations. Upon addition of EKMax™ a low molecular weight protein band is visible corresponding to the cleaved his-tag.

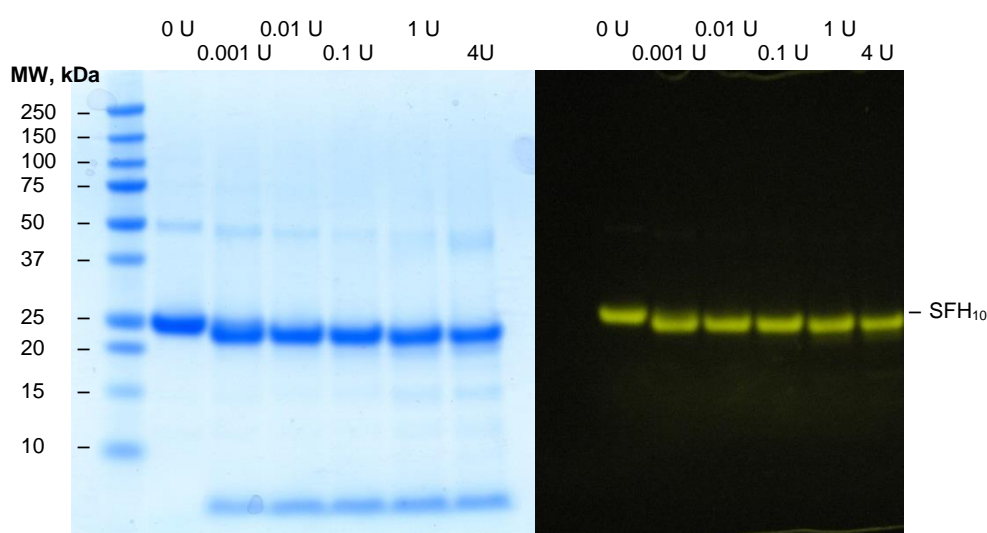


Figure 12. (Left) SDS Page of SFH₁₀ cleaved with different amounts of EKMax™. The protein was labeled with SNAP-Vista® Green prior to being run on the gel. (Right) Same SDS-Page gel before staining and excited with blue light.

SFH₁₀-647 was reacted with EKMax™ using the 20:0.1 ratio. A SEC was used to isolate the different components of the mixture. During this step, absorbance at 647 nm was monitored to detect the cleaved SFH₁₀-647 (figure 13) showing this protein is eluted at 10 mL. This elution volume corresponds to particles with 50 kDa, double the size of the protein of interest. This indicates the protein is organized into dimers. A second elution peak at 27 mL is visible when monitoring absorbance at 280 nm. This elution peak matches the low molecular weight protein band visible on the SDS-PAGE gels (figure 12), thus corresponding to the cleaved his tag.

Protein concentration of the sample was assessed by measuring the absorbance at 647 nm (protein concentration = 3.27 µM). The absorbance at 647 nm can be

correlated to the concentration of fluorophore in solution using Lambert-Beer law, which in turn can be related to the protein concentration using the DOL measured for the non-cleaved protein (64.58 %).

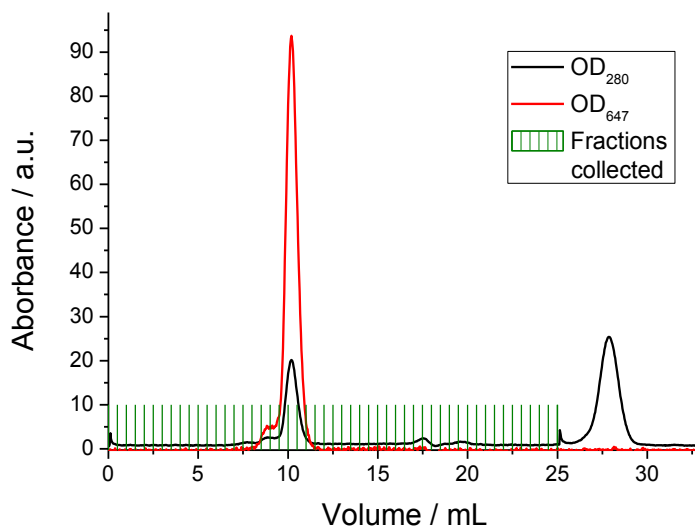


Figure 13. Chromatogram of the separation of the different components of the mixture after cleavage of the his-tag from SFH₁₀-647.

2.4. Conclusion

This chapter reported the expression and purification of H₆-EGFP, followed by the characterization of the sample. The protein was purified in two steps: first by IMAC, relying on the affinity of the Ni-NTA motifs on the column for the His-tag, and then by SEC, separating the protein of interest from impurities with very different sizes.

The second part reported in this chapter describes the expression and purification of SFH₁₀. This fusion protein is morphologically different from EGFP and it can be labeled with a BG derivative containing a fluorophore. Due to some of the impurities in solution showing affinity to the Ni-NTA motifs, SFH₁₀ was purified by gradient IMAC. After purification of SFH₁₀, the protein was labeled with SNAP-Surface[®] 647. The labeled protein was characterized by SDS-Page gel and by determining the DOL. This parameter provides information on the amount of fluorophore in relation to the amount of protein.

The final part of the chapter reports the cleavage of the His-tag from SFH₁₀-647. SFH₁₀ was labeled prior to the cleavage to ensure the DOL would be the same in the full and the cleaved proteins.

Chapter 3.

***Analysis of protein binding to
polystyrene microparticles***

3.1. Introduction

3.1.1. Aim of the project

In this chapter, the use of polystyrene microspheres to immobilize his-tagged proteins to solid support is reported and two different techniques used to analyze this interaction. While microparticles are an interesting tool allowing an easy immobilization of proteins in solution using simple procedures it is important to comprehend the system, its advantages and its limits. With this in mind, functionalized particles were analyzed using fluorescence spectroscopy and fluorescence microscopy while comparing both approaches.

3.1.2. Polystyrene microspheres

While 2D surfaces have been more extensively applied as biosensors, microparticles provide a platform which is easier to transpose current techniques to. Microparticles can be analyzed in solution using techniques such as dynamic light scattering or flow cytometry, or immobilized on a surface so they can be studied using fluorescence microscopy^[1]. By functionalizing the particles separately with different proteins this platform also offers the possibility of multiplexing, making microparticles arrays a economic and easily prepared platform to study protein-protein interactions or protein-drug interactions^[1,35]. Furthermore, by varying the particles' size or doping agents (incorporated dyes), it is easy to track particles individually through several functionalization steps.

Proteins can be immobilized on the particles' surface by physisorption. Nonetheless, as previously stated (refer to chapter 1), proteins adsorbed this way have a random orientation, usually resulting in a decreased biological activity. By coating the particles with target molecules, this problem can be circumvent ^[1,7]. Polystyrene microparticles with different coatings are commercially available. These particles are usually used for protein purification, to remove certain molecules from solution or simply as size standards to calibrate equipment. However the possibility of protein multiplexing makes microparticles a promising platform to apply to bioanalytics^[36]. In fact, some companies have started developing bead arrays (most of which in solution) to DNA screening.

3.1.3. Nitriloacetate complexes

Transition metal complexes have been used as chemosensors or to study metallo enzyme function and supramolecular self-assembly. Transition metals act as a Lewis acid and can interact with a variety of Lewis basic functional groups. This interaction goes beyond a simple electrostatic interaction. The transition metal shows intrinsic selectivity towards the nature of the donor. This selectivity is justified by the hard soft acid base (HSAB) principle stating that hard acids favor the interaction with hard bases, while soft acids prefer soft bases^[21,37,38].

Especially when immobilizing metals on a surface, it is important to make the right choice of ligand to use. While a single coordinative bond may provide sufficient binding strength to form a stable complex, it does not provide enough stability to retain the metal cation. The selected immobilized ligand should be polydentate to exclude competing ligands, possibly the solvent. The choice of what metal ion to use also has an impact on the system as different metals also result in different affinities. (Table1)

Table 2. Binding constants of different metal ion toward NTA measured at 20°C. Adapted from [21].

ion	equilibrium	log <i>K</i> (25 °C)	ion	equilibrium	log <i>K</i> (25 °C)
Fe ²⁺	ML/M•L	8.33 ^a	Fe ³⁺	ML/M•L	15.9
	ML ₂ /M•L ²	12.8 ^a		ML ₂ /M•L ²	24.3 ^a
Co ²⁺	ML/M•L	10.38	Cd ²⁺	ML/M•L	9.78
	ML ₂ /M•L ²	14.33		ML ₂ /M•L ²	14.39
Ni ²⁺	ML/M•L	11.5	Zn ²⁺	ML/M•L	10.66
	ML ₂ /M•L ²	16.32		ML ₂ /M•L ²	14.24
Cu ²⁺	ML/M•L	12.94	Al ³⁺	ML/M•L	11.4
	ML ₂ /M•L ²	17.42			

^a Measured at 25 °C.

NTA complexes have been used as a chelate for several metal ions. Although the most common application is in IMAC to purify His-tagged proteins, NTA complexes have also been applied to protein immobilization on micro- or nanoarrays^[21].

NTA is a tetradentate ligand being able to establish four coordination bonds to the metal ion. When bound to Nickel (II), favoring an octahedral geometry, there are two free binding sites in a *cis* position. As imidazole groups have a high affinity for Ni²⁺, reason why his-tagged proteins can be attached to the complex. And, by using a high concentration of molecular imidazole, the immobilized protein can be released. An alternative to release the protein is by chelating the central metal ion, usually with EDTA. As EDTA is a hexadentate ligand, it has a higher affinity than NTA, thus

capturing the metal ion from the NTA complex and releasing the bound protein at the same time^[34,36].

3.2. Materials and methods

3.2.1. Functionalization of polystyrene microparticles in solution

To prepare the calibration curve of the absorbance versus the concentration of polystyrene microparticles coated with Ni-NTA (NiNTA-PPsMPs)(Kisker Biotech) , the particles were diluted in PBS directly from the stock.

NiNTA-PPsMPs were functionalized by taking 100 μL NiNTA-PPsMPs from stock, diluting to 1 mL with PBS and washing twice with PBS. After the washing steps, NiNTA-PPsMPs concentration was determined using OD_{600} and 0.2 mg NiNTA-PPsMPs were incubated with different concentrations of H₆-EGFP in PBS for 2 hours, in the dark, at room temperature. The samples were then washed twice with PBS. The controls were prepared by incubating NiNTA-PPsMPs with H₆-EGFP in PBS supplemented with 100 mM imidazole.

3.2.2. Immobilization of Polystyrene Microparticles on a glass surface

To prepare the functionalized glass surface, a glass slide (VWR) was first washed with MQ water, Ethanol and Acetone and dried under N₂ flow. Then, it was Ni Plasma etched for 180s, covered with 100 $\mu\text{g mL}^{-1}$ poly-L-lysine bromide for 2 min and rinsed with deionized water for 10 s.

NiNTA-PPsMPs were first diluted in deionized water and then immobilized onto the glass surface by covering the surface with the particles for 30 min at room temperature. Non-immobilized particles were removed by rinsing the glass slide with a stream of deionized water for 10 s. NiNTA-PPsMPs were functionalized by covering the glass slide with H₆-EGFP in PBS, in the dark, at room temperature, for 30 min. Excess of H₆-EGFP was removed by rinsing for 10 s with deionized water.

Elution of the bound protein with imidazole or EDTA was accomplished by immersing the particles in PBS containing either 500 mM imidazole or 500 mM EDTA for 30 min, in the dark, at room temperature and then rinsing with MQ water for 10 s.

3.2.3. Absorbance spectra

Absorbance spectra were recorded using a Cary 50 Bio UV-Vis spectrophotometer. The absorbance spectra were monitored from 250 nm to 700 nm with 1 nm increment using PBS as blank.

3.2.4. Fluorescence spectra

Excitation and emission spectra of H₆-EGFP samples were measured on a Fluorolog Spectrofluorimeter (HORIBA, Jobin Yvon). Samples were excited at 488 nm (slit 3 nm) and emission spectra were monitored between 500 nm and 700 nm (slit 3 nm), with integration time of 0.5 s nm⁻¹ and with an increment of 1 nm.

3.2.5. Fluorescence microscopy

Immobilized microparticles were imaged using a Leica DM5500 B microscope equipped with a Leica EL600, mercury metal halide lamp bulb.. Fluorescence images were taken with a Leica GFP filter (to monitor H₆-EGFP) and a Chrome Cy5 filter (to monitor SFH₁₀-647). The samples were imaged in PBS after functionalization and after elution.

The images were analyzed with ImageJ. For the analysis of the particles, a mask was created around each particle using the brightfield (DIC) image, which was transposed to the GFP filter image. This allows the analysis of each particle individually.

The fluorescence intensity (intensity) of the particles was analyzed in relation to the background, as follows:

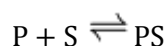
$$\text{intensity} = I_{F,\text{particles}} - I_{F,\text{background}}$$

Where $I_{F,\text{particles}}$ is the mean fluorescence intensity of the particles and $I_{F,\text{background}}$ is the fluorescence intensity of the background.

3.3. Results and Discussion

3.3.1. Analysis of polystyrene microparticles by fluorescence spectroscopy

Usually, when the adsorption of a molecule occurs via a chemical reaction, a monolayer is formed. The formation of a monolayer on surface can be described by



where S is the free binding sites on the surface, P is adsorbate and PS is the complex formed between the surface and the adsorbate^[39,40]. Writing the equilibrium equation for this reaction

$$K = \frac{[PS]}{[P][S]}$$

where K is the equilibrium constant. In the case of the adsorption of H₆-EGFP to NiNTA-PPsMPs, the amount of bound protein is directly proportional to the surface area available, which in turn, is proportional to the concentration of particles in solution. When working with low concentrations of particles, fluctuations on the concentration of particles translate in a variation of the amount of bound protein. The loss of particles during the washing steps or simply non-specific binding to the walls of the containers also influence the surface area available.

Preliminary experiments showed that absorbance is directly proportional to the concentration of polystyrene microparticles in solution. Thus, to monitor the concentration of NiNTA-PPsMPs, absorbance spectra of different concentrations of NiNTA-PPsMPs were recorded (figure 14). To ensure the presence of H₆-EGFP does not contribute to absorbance of the samples of NiNTA-PPsMPs functionalized with the protein, it was decided to monitor OD₆₀₀ to determine the concentration of NiNTA-PPsMPs (figure 15). The results show OD₆₀₀ is directly proportional to the concentration of NiNTA-PPsMPs between 0.01 mg mL⁻¹ and 0.63 mg mL⁻¹.

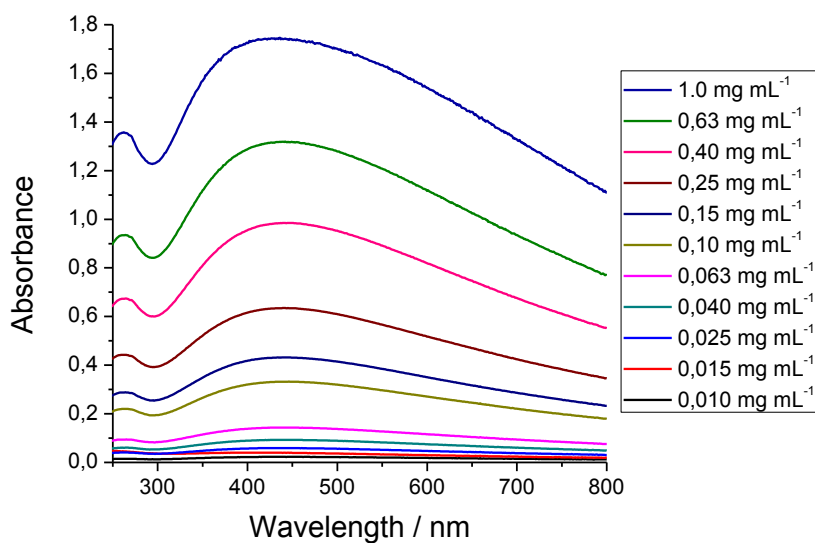


Figure 14. Absorbance spectra of different concentrations of NiNTA-PPsMPs.

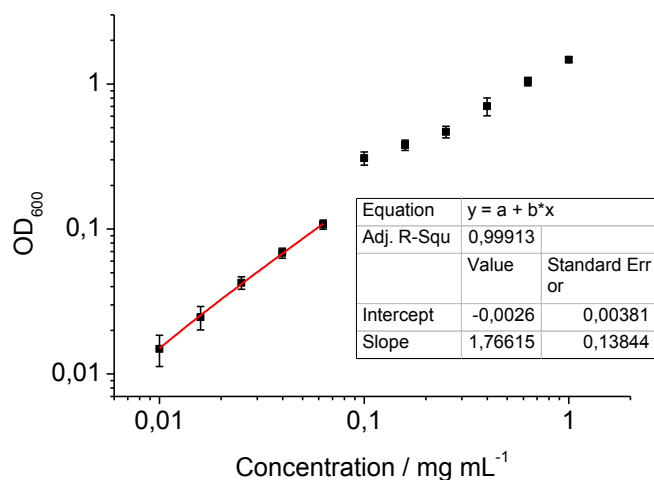


Figure 15. Calibration curve of the absorbance versus the concentration of NiNTA-PPsMPs. The error bars correspond to the standard deviation from 3 independent samples.

In order to demonstrate the concentration of NiNTAPPsMPs has no influence over the emission of the sample at 510 nm (when exciting at 488 nm), emission spectra of different concentrations of NiNTA-PPsMPs (from 0.01 mg mL⁻¹ to 0.063 mg mL⁻¹) were measured (figure 16). These samples showed the same fluorescence intensity measured in the absence of NiNTA-PPsMPs (PBS).

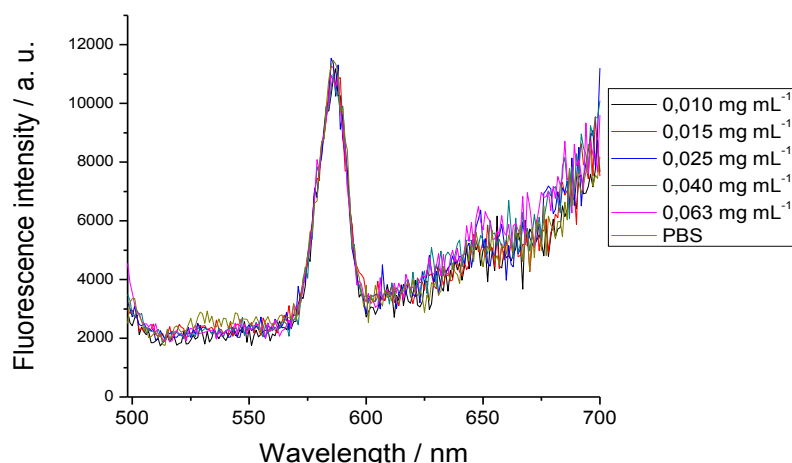


Figure 16. Emission spectra ($\lambda_{\text{ex}}=488$ nm) of different concentrations of NiNTA-PPsMPs suspended in PBS.

Using the emission signal at 510 nm (exciting at 488 nm), the binding curve of H₆-EGFP onto NiNTA-PPsMPs was determined (figure 17). Analyzing the mean signal, there is an increase of bound protein with the concentration of H₆-EGFP. As the amount of bound protein does not reach a plateau as expected for the formation of monolayers following Langmuir isotherm^[39,40], the samples have not been saturated yet. The samples also show a high standard deviation of the emission signal for independent samples, indicating this system lacks sensitivity.

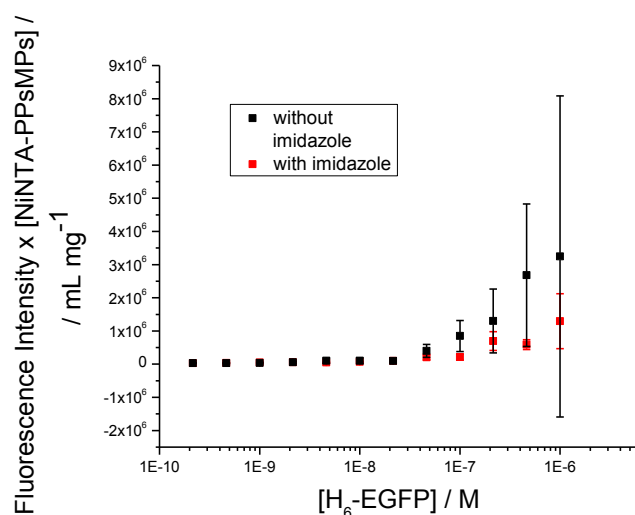


Figure 17. Binding curve of H₆-EGFP onto the surface of NiNTA-PPsMPs. H₆-EGFP was added to 0.2 mg mL⁻¹ NiNTA-PPsMPs.

To demonstrate the specific binding of H₆-EGFP to the Ni-NTA motifs, the binding curve of H₆-EGFP to NiNTA-PPsMPs was determined in the presence of 100 mM imidazole. Comparing both binding curves of H₆-EGFP to NiNTA-PPsMPs (in the absence or presence of imidazole) when in the absence of imidazole there is a 2- to

3-fold lower amount of H₆-EGFP on the NiNTA-PPsMPs. Imidazole competes with H₆-EGFP for the binding sites to the Ni-NTA motifs and in the presence of 100 mM imidazole, the equilibrium favors the formation of the complex with imidazole, thus blocking the protein from interacting with the Ni-NTA motifs.

3.3.2. Immobilization and functionalization of polystyrene microparticles on a glass surface

A different way to measure the binding of H₆-EGFP is by fluorescence microscopy. Fluorescence microscopy requires the particles to be immobilized on a surface. The glass surfaces were functionalized with PLL prior to the immobilization of NiNTA-PPsMPs. This peptide is positively charged, thus interacting with the negative charge of the NiNTA-PPsMPs and allowing them to remain bound to the surface (figure 18).

Different dilutions of NiNTA-PPsMPs in deionized water (from 50 mg mL⁻¹ to 0.05 mg mL⁻¹) were deposited on the surface to assess the optimal concentration to use. It is important to tune the concentration of particles on the surface in order not to hinder the analysis. The density of immobilized particles must be high enough to allow a significant number of particles to be analyzed and, at the same time, it must be low enough so the particles can be easily analyzed individually. The results (figure 18) show that 0.5 mg mL⁻¹ is the optimal concentration. While lower dilutions show too many particles on the surface and higher dilutions show too few immobilized particles, 0.5 mg mL⁻¹ NiNTA-PPsMPs show the right amount of particles on the surface. Therefore it was decided to use a concentration of 0.5 mg mL⁻¹ NiNTA-PPsMPs on further experiments.

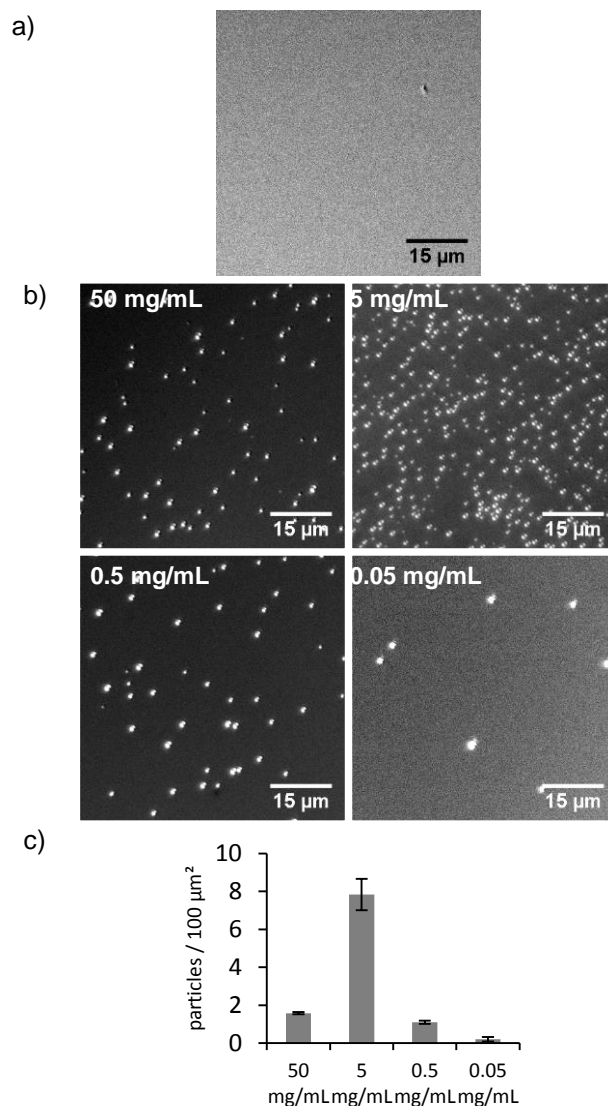


Figure 18. (a) Different concentrations of NiNTA-PPsMPs immobilized on the glass slide. (c) Density of particles on the glass slide for different NiNTA-PPsMPs concentrations. Error bars correspond to the standard deviation of the density of particles on the glass surface.

After functionalizing the surface with NiNTA-PPsMPs, the slides were incubated with different concentrations of H₆-EGFP (1 nM, 10 nM, 100 nM or 1000 nM). Fluorescence images recorded in the GFP filter images show that the amount of bound protein is positively correlated to the amount of protein added (figure 19). For the samples functionalized with 1 nM H₆-EGFP no intensity was detected. Similarly to the results obtained by fluorescence spectroscopy, the amount of bound protein has not yet stabilized, thus the NiNTA-PPsMPs are not fully saturated.

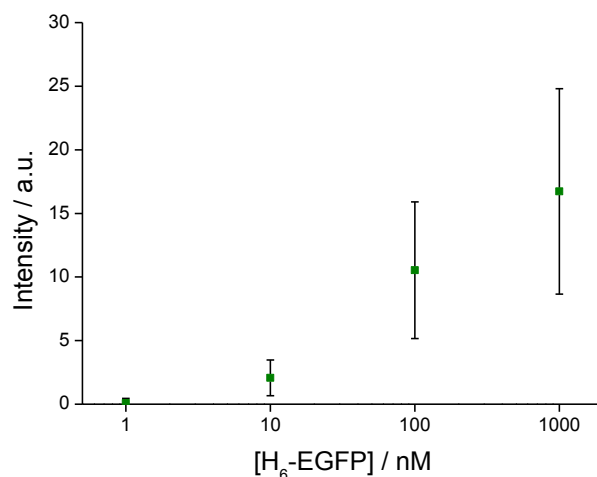


Figure 19. Fluorescence intensity of different concentrations NiNTA-PPsMPs in relation to the fluorescence intensity of background as measured by fluorescence microscopy.

The specific binding of H₆-EGFP to the Ni-NTA motifs was determined by incubating the glass slide functionalized with H₆-EGFP with EDTA (figure 20) or imidazole (figure 21). Fluorescence micrographs recorded in the GFP channel show that upon addition of 500 mM EDTA the intensity of the samples functionalized with 100 nM or 1000 nM H₆-EGFP is halved (figure 22), while for the sample functionalized with 10 nM H₆-EGFP no decrease was detected. Upon addition of imidazole, the intensity of the samples functionalized with 100 nM and 1000 nM H₆-EGFP increases, while the intensity for the samples functionalized with 1 nM or 10 nM show no variation (figure 22). Despite the increase of the intensity verified for the samples functionalized with 100 nM or 1000 nM H₆-EGFP upon elution with imidazole, the line scans of the images of these samples before and after elution show a decrease of the fluorescence intensity of the NiNTA-PPsMPs upon incubation with imidazole. However, these images show a higher decrease of the fluorescence intensity of the background in comparison to the decrease of the fluorescence intensity of the NiNTA-PPsMPs, thus resulting in a higher intensity upon incubation with imidazole.

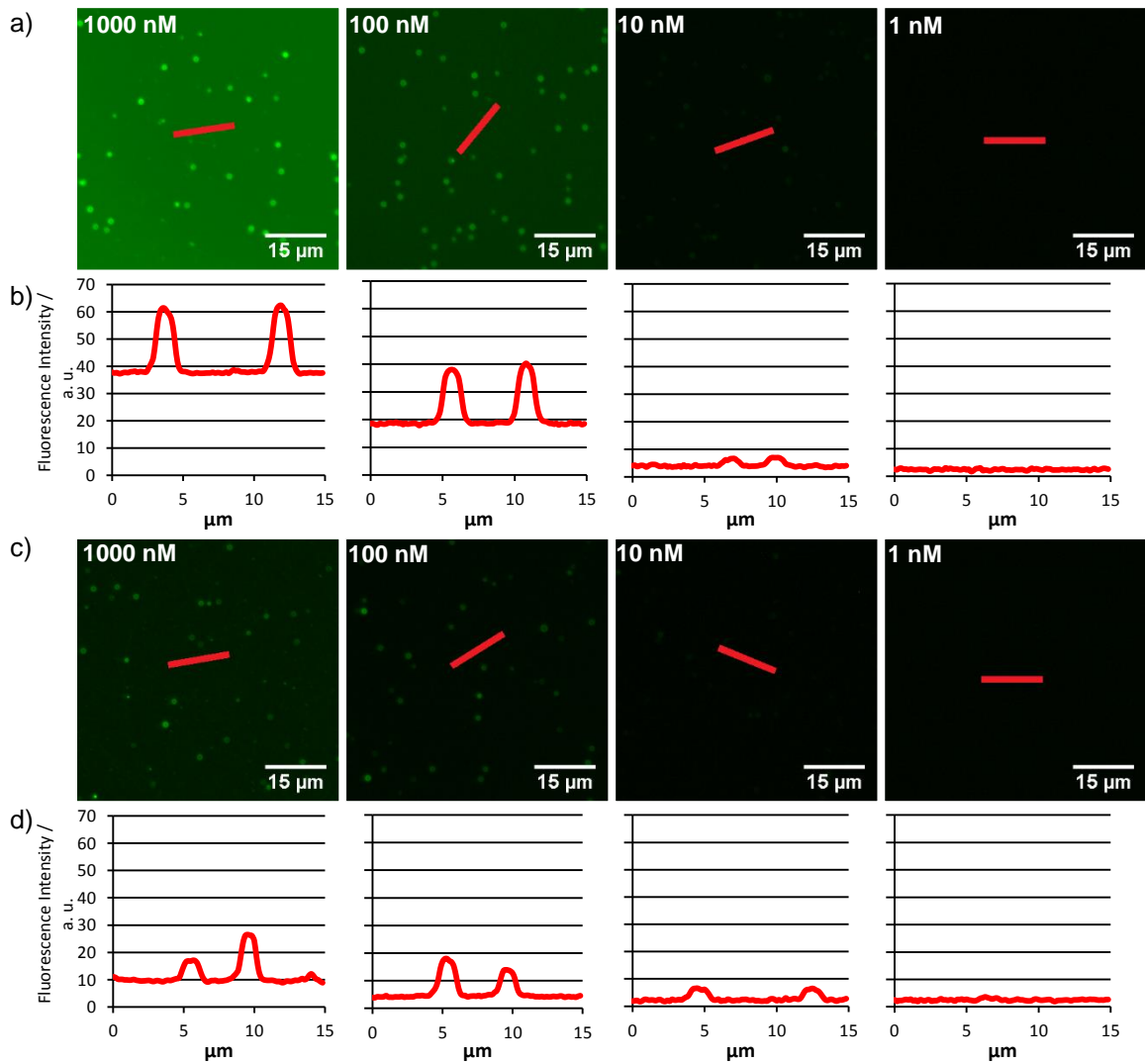


Figure 20. (a) Fluorescent microscopy images (GFP filter) of immobilized NiNTA-PPsMPs functionalized with different concentrations of H₆-EGFP prior to elution with EDTA. The red line corresponds to the area the line scans were taken from. (b) Line scans of the images shown on a). (c) Fluorescent microscopy images (GFP filter) of immobilized NiNTA-PPsMPs functionalized with different concentrations of H₆-EGFP after elution with 500 mM EDTA. The red line corresponds to the area where the line scans were taken from. (d) Line scans of the images shown on c).

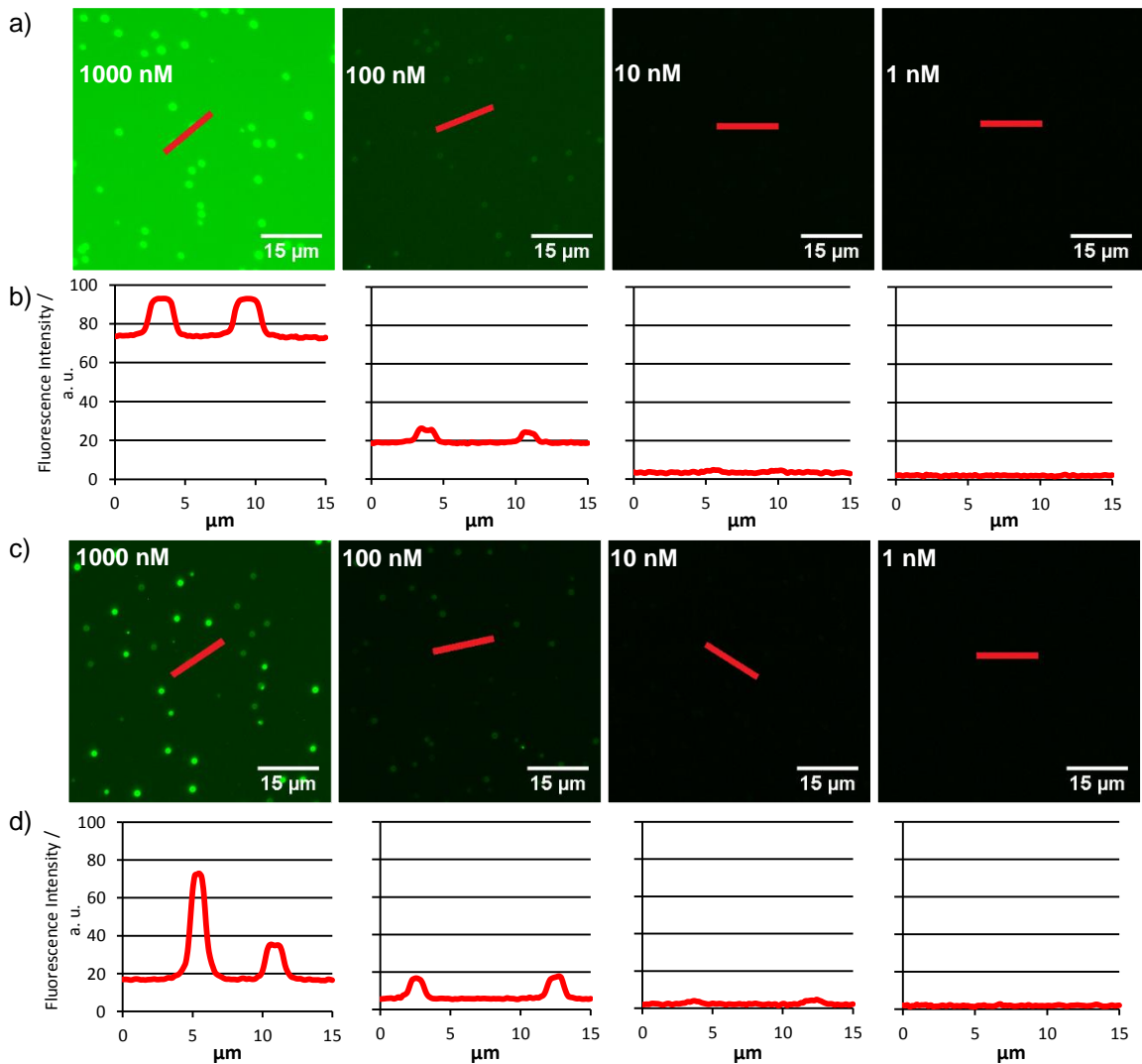


Figure 21. (a) Fluorescent microscopy images (GFP filter) of immobilized NiNTA-PPsMPs functionalized with different concentrations of H₆-EGFP. The red line corresponds to the area the line scans were taken from. (b) Line scans of the images shown on a). (c) Fluorescent microscopy images (GFP filter) of immobilized NiNTA-PPsMPs functionalized with different concentrations of H₆-EGFP after elution with 500 mM Imidazole. The red line corresponds to the area where the line scans were taken from. (d) Line scans of the images shown on c).

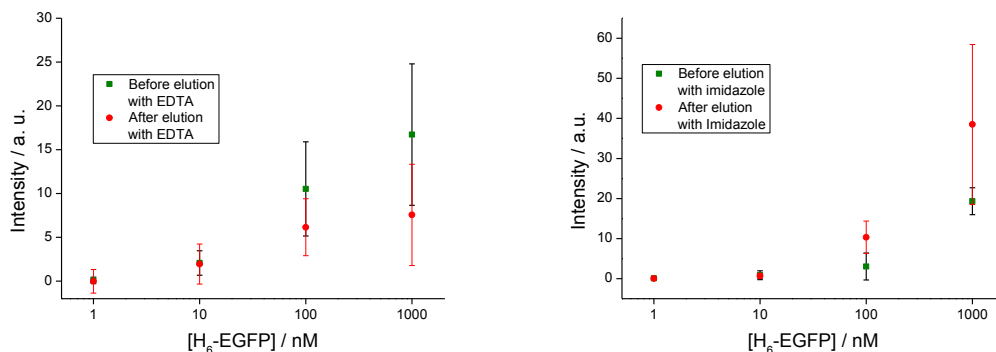


Figure 22. Fluorescence intensity of NiNTA-PPsMPs with different concentrations of H₆-EGFP prior and after elution. On the left 500 mM EDTA was used to elute the protein and on the right it was eluted with 500 mM imidazole.

3.3.3. Immobilization of functionalized polystyrene microparticles on a glass surface

A different approach aiming at immobilizing different proteins on the same glass slide is to functionalize NiNTA-PPsMPs with protein while in solution and then immobilizing the functionalized particles on the glass surface. By separately functionalizing NiNTA-PPsMPs with different proteins and mixing them prior to the immobilization of the particles onto the surface it is possible to immobilize different proteins on the glass surface. The proof-of-concept is shown in figure 23. NiNTA-PPsMPs were separately functionalized with 100 nM H₆-EGFP and 100 nM SFH₁₀-647 and immobilized on a PLL coated glass surface. H₆-EGFP and SFH₁₀ have a pI of 6.13 and 6.16, respectively, thus, at pH 7.4 the proteins are negatively charged. As upon functionalization of the NiNTA-PPsMPs, these negatively charged proteins are covering the surface of the particles, the positively charged PLL is able to interact electrostatically with the protein coating of the particles and immobilize them. Figure 23 shows the functionalized NiNTA-PPsMPs remain on the surface even after extensive rinsing with deionized water.

Line scans from the fluorescence micrographs recorded with the GFP (to monitor H₆-EGFP) and Cy5 (to monitor SFH₁₀-647) were normalized between 0 and 1 (figure 23, b) as the aim of this experiment is to show the proof-of-concept of the use of NiNTA-PPsMPs for protein immobilization and not to quantify the amount of protein immobilized. Particles functionalized with different proteins can be clearly identified on the different channels (GFP and Cy5) and no transfer of proteins from different beads is detected.

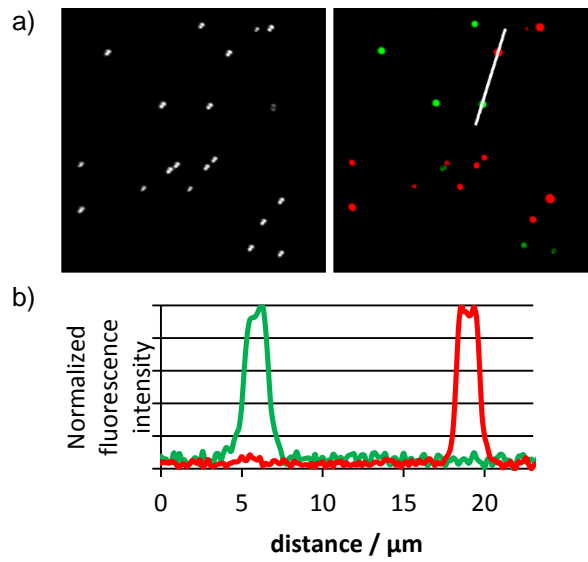


Figure 23. (a) Brighfield (DIC) (left) and fluorescent microscopy (GFP filter in green and Cy5 filter in red) images of immobilized NiNTA-PPsMPs previously functionalized with H₆-EGFP or SFH₁₀-647. The white line corresponds to the area where the line scans were taken from. (d) Line scans of the fluorescent microscope images taken with the GFP filter (—) and the Cy5 filter (—).

3.4. Conclusion

In this chapter, I have reported the immobilization of H₆-EGFP on NiNTA coated polystyrene microparticles.

The first approach dealt with the protein immobilization of while the particles are suspended in solution and analysis by fluorescence spectroscopy. The binding curve of H₆-EGFP was determined using this method. As the amount of bound protein has not stabilized at the higher concentrations of H₆-EGFP, as expected for the formation of monolayers, the NiNTA-PPsMPs are not fully saturated. Analysis by fluorescence spectroscopy showed a low sensitivity and the amount of bound protein is inconsistent among independently prepared samples.

The second approach is to immobilize the particles on a surface prior to their functionalization and analyze them using fluorescence microscopy. The negative charge of the Ni-NTA motifs on the surface of NiNTA-PPsMPs allows these particles to remain immobilized on a PLL functionalized glass surface even after extensive rinsing with deionized water. Analysis by fluorescence microscopy showed a higher sensitivity than fluorescence spectroscopy analysis. However, elution with imidazole has shown the background has a high influence on the analysis and needs to be considered in order to comprehend the results obtained.

The third approach followed aims at the production of protein microarrays. By separately functionalizing the particles in solution, mixing them and then immobilizing the particles on a glass surface, it is possible to immobilize different proteins on a single glass surface. Immobilization of the particles relies on the electrostatic interaction between the charged proteins on the NiNTA-PPsMPs and a PLL layer coated on the glass surface. Analysis by fluorescence microscopy allows the clear distinction between the NiNTA-PPsMPs functionalized with H₆-EGFP or SFH₁₀-647 and no protein transfer is detected between particles functionalized with different proteins. This approach provides an easy approach towards the fabrication of protein arrays. The use of dye-doped microparticles might provide an easy way to track different proteins without requiring the use of fluorescently labeled proteins. Furthermore, the use of nanoparticles instead of microparticles provides a route towards the fabrication of protein nanoarrays. The ability to immobilize proteins on microparticles may be extended to a wide range of applications including the analysis of protein-protein interactions.

Chapter 4.

Directed protein immobilization: approaching nanoscale protein multiplexing

4.1. Introduction

4.1.1. Aim of the project

In this chapter, I demonstrate the use of electropolymerization of a PPy film onto gold micro- and nano-electrodes and its subsequent functionalization as a versatile route towards protein multiplexing. It is shown that by activating each electrode individually we can select the location of the film and use it to immobilize proteins. It is also reported the use of electric fields to enhance protein adsorption. Immobilization of the H₆-EGFP and SFH₁₀-647 were monitored by fluorescence microscopy.

4.1.2. Conducting polymers

Protein immobilization on electrodes is of special interest to the development of biosensors. In fact, biosensors based on electrochemical transduction show a high adaptability, are easily fabricated with a high throughput and are usually simple to use even in complex samples^[9].

Even though this concept was first demonstrated in 1962 by Clark and Lyons^[41] and despite all the improvements made so far, the procedure of immobilizing biomolecules on a conductive surface still is an essential step in the performance of the device^[42].

Electrogeneration of polymer films is a versatile approach towards protein multiplexing allowing a highly controllable, reproducible, low-cost and easily scaled up manufacturing process^[42]. Furthermore, the electrochemical generation of polymer films can be done over a variety of conducting or semiconducting surfaces which, in turn, can be fabricated using established semi-conductor fabrication procedures allowing an easy transition to the industry.

The most common strategy for immobilizing proteins in polymer films is by their entrapment within the film^[42-44]. Biomolecules in the vicinity of the electrode are incorporated into the growing film. This immobilization procedure allows the immobilization of a wide variety of biomolecules which can still retain the biological activity without being covalently attached to the surface. Despite the advantages of the electrochemical entrapment of biomolecules, the drawbacks may be just as big. This approach requires high concentration of monomer (0.05 to 0.4 mol L⁻¹) and biomolecules (0.2 to 3.5 mg mL⁻¹). The latter may be very expensive or not available in such large concentration, hampering the production in large scale. Also, the steric

constraints by the polymer film reduce accessibility to the immobilized molecules resulting in a reduced activity^[42].

The easy N-substitution of pyrrole can also be used to immobilize protein on the film's surface. By chemically attaching an affinity-tag to pyrrole, fusion proteins can be selectively immobilized^[42]. Gondran *et al* have generated a NTA chelator film that was used to immobilize His-tagged molecules^[45]. The same group later used a similar approach to attach biotinylated biomolecules^[46]. The avidin-biotin linkage has also been used to immobilize proteins on polypyrrole films. Rossi *et al* first used a biotinylated derivate of pyrrole to generate such a polymeric film^[47].

By successively generating films with different properties, electropolymerization can also allow protein multiplexing on different regions of an electrode array. This was first shown by Reed *et al* who generated films with different properties in order to chemically attach different fluorophores.

4.1.3. Ion migration within an electric field

The motion of particles (originally clay granules) within an electric field (known as electrophoresis) was first observed in 1807 by Reuss and this phenomenon has been extensively studied^[49,50]. In 1937, Tiselius used this process as an analytical and preparative separation tool^[51]. Since then, electrophoresis has grown to be recognized as the most effective separation tool.

The transport of current through an electrolytic system is carried out by ions or, more comprehensively, charged particles. In solution, the charge of a macromolecule, such as a protein, arises by the ionization of the functional groups contained by the molecule. These groups may result in either positive or negative charges each one contributing to the net charge of the protein. In an acidic environment, the functional groups tend to be protonated, thus resulting in a positive net charge, while in a basic environment the opposite is true. At a certain pH, the contribution from the positive and negative functional groups should be the same and the net charge of the protein is null. This corresponds to the isoionic point. Despite the protein bearing no net charge at the isoionic point, it does not mean it will have no electrophoretic mobility (usually called isoelectric point). The surface charge of a protein leads to the adsorption of free ions (of opposite charge to the surface charge) onto its surface, forming a double layer which may modify its net effective charge^[51].

When placed in an electric field, molecules are subject to a number of different forces and, as a steady state is reached, the protein migrates at a constant velocity. We may consider four forces act over the particle (figure 24). The most important is the

electrophoretic attraction resulting from the charge of the particle and the strength of the applied electric field. There is also the Stokes friction which corresponds to the viscous drag. Another important slowing effect is the electrophoretic retardation. This effect is related to the double layer surrounding the particles. As the outer layer is composed of ions with the opposite charge of the protein, they are attracted in the opposite direction of the particle, thus slowing its movement. The final effect is known as relaxation retardation. This effect results from the different movements of the particle and its surrounding ions. This movement distorts the ionic surroundings of the particle so it is no longer in the centre of the electric environment^[51].

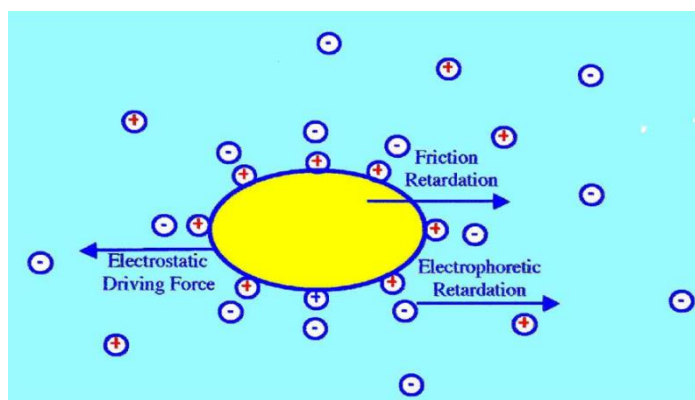


Figure 24. Schematic representation of the formation of a double layer surrounding the particle and the major forces which act over it. Adapted from [51].

As charged particles move in solution towards an electrode, this results in an upconcentration of the molecules at the electrode. In principle, it should be possible to use this upconcentration to increase the amount of adsorbed particles onto an electrode. It should also be possible to prevent proteins adsorption onto the surface of the electrode by applying an electric field of opposite sign and therefore electrostatic repulsion. By combining these two effects, it should be possible to control the adsorption of different particles on different electrodes of an array.

Wong et al have shown the application of such principles by controlling the hybridization of oligonucleotides onto probe functionalized gold electrodes^[52]. However, there are no reports showing directed protein adsorption on the surface of electrodes using electric fields.

In this chapter, I show how the use of an organic conducting polymer film, polypyrrole, in conjugation with an electric field allows the enhancement of protein adsorption onto the polymer surface while allowing the proteins to remain correctly folded.

4.2. Materials and Methods

4.2.1. Microelectrode arrays

Micro-/ nanoelectrode arrays (figure 25) were fabricated by Jesper Nygård's group using either e-beam lithography or photolithography. The electrodes are made of gold (Au) deposited on a Titanium surface on a SiO_2 surface. Three different designs of the array have been used as shown in figure 25, b. The first design used (figure 25, b,1) is composed of 8 μm wide electrodes with 10 μm wide tip and was fabricated using e-beam lithography. The second design used (figure 25, b,2) is composed of 5 μm wide electrodes and was fabricated by photolithography. The third design used (figure 25, b,3) is composed of 5 μm electrodes with small indentations at the tip which go as low as 80 nm. Three electrodes have been extended to form 300 nm wide electrodes designed in a spiral.

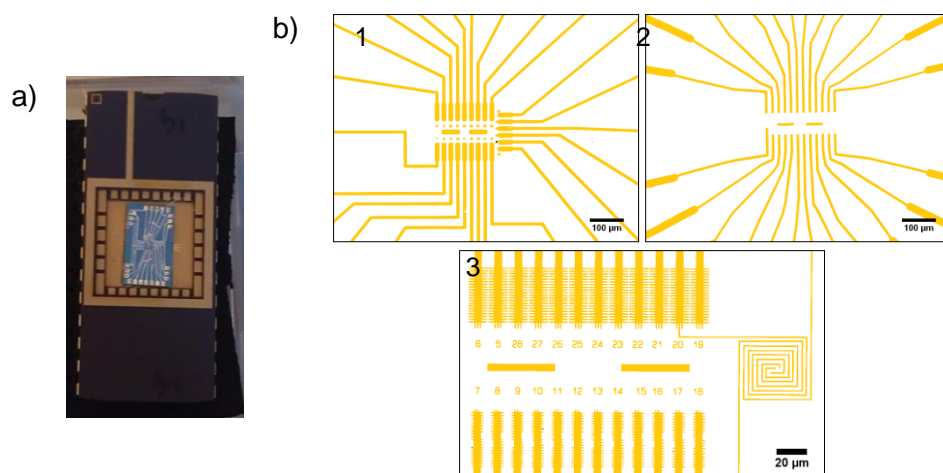


Figure 25. (a) Image of one of the electrode arrays used. (b) Schematic representation of the different electrodes' layouts used.

4.2.2. Assembly of the electrochemical cell

The electrochemical cell used is a small plastic container placed on top of the electrode array and in which the electrolyte solution can be placed. The cell is covered by a plastic lid through which the reference and counter electrodes can be inserted. Before mounting the electrochemical cell, the electrode array was rinsed with deionized water, 70% ethanol, and acetone. It was dried with a gentle stream of N_2 . The plastic chamber was washed with MQ water and 70% ethanol and dried under N_2 . Only then, were the different components assembled. Both the reference electrode and the counter electrode were Platinum wires.

4.2.3. Electropolymerization of the polypyrrole film

In order to polymerize the PPy film, the electrochemical cell was filled with freshly prepared 10 mM NaCl, 0.1 M Pyrrole. To prevent oxidation from O₂, N₂ was purged into the electrochemical cell for 5 min. Then, 0.7V were applied onto the working electrode until the deposited charge equaled -5×10^{-5} C. The polymerization solution was removed by extensively rinsing the electrode array with deionized water.

4.2.4. Functionalization of the electrodes

After generation of the PPy film, the electrode was grounded for 10 min, while immersed in PBS, to ensure no residual charges remained in the surface of the PPy film.

To functionalize the electrodes, the chamber was filled with 100 nM protein (H₆-EGFP or SFH₁₀-647) diluted in PBS. N₂ was purged into the cell for 5 min to avoid oxidation by O₂. Different potentials and times were investigated to optimize conditions for protein immobilization on the PPy film. To remove excess protein, the chamber was rinsed with PBS and washed with 0.001% Tween 20 in PBS for 10 min and rinsed with PBS again.

4.2.5. Fluorescence microscopy

Microscopy images of immobilized microparticles were taken using a Leica DM5500 B microscope equipped with a Leica EL600, mercury metal halide lamp bulb. Samples were imaged with a Leica GFP filter (to monitor H₆-EGFP) and a Chrome Cy5 filter (to monitor SFH₁₀-647). The electrodes were imaged in PBS after prior and after polymerization of the PPy film and after functionalization.

The images were analyzed with ImageJ. Fluorescence intensity was determined according to:

$$\text{Intensity} = I_{F,n} - I_{F,0}$$

Where $I_{F,0}$ and $I_{F,n}$ corresponds to the fluorescence intensity of the PPy film prior and after functionalization, respectively.

4.3. Results and Discussion

The functionalization strategy used in this project involves the electropolymerization of a PPy film on a gold microelectrode, followed by immobilization of the proteins onto the surface of the PPy film (figure 26). Using this approach, it is possible to gain control over the area functionalized, as the PPy film is generated only on top of the working electrode.

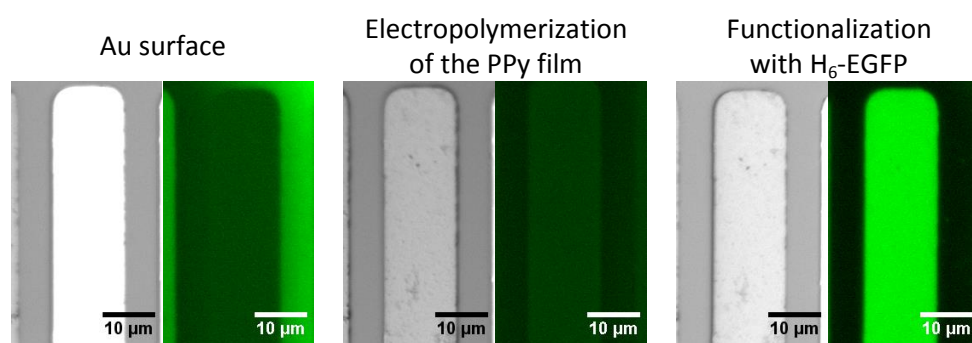


Figure 26. Brightfield (DIC) and GFP filter images of a electrode throughout the functionalization process.

The functionalization step revolves around the use of electrical fields to direct proteins onto the electrodes. Figure 27 shows that when a potential is applied (600 mV) on the working electrode, the amount of protein on the PPy film is nearly 2-fold higher than when the electrode is disconnected from the electric circuit and therefore in open-circuit. By applying a potential onto an electrode, the movement of the ions, including macromolecules, such as proteins in solution is promoted in the direction of the electrodes. This creates a protein upconcentration at the electrodes, thus promoting the binding to the surface and requiring a smaller amount of protein than would be necessary otherwise.

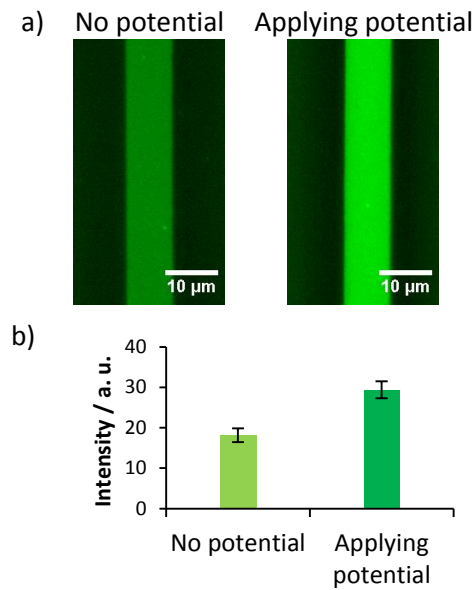


Figure 27. (a) GFP filter images of gold electrodes functionalized on an open-circuit or when applying a potential (600 mV). (b) Increase in fluorescence intensity in relation to the non-functionalized PPy film for both conditions.

When trying to functionalize gold electrodes in the absence of a PPy film, no fluorescence signal from the protein is detected as seen in figure 28. This might mean that the protein loses its tertiary structure and, therefore, its function. Another possible explanation for not detecting any signal from the bound protein is that the gold quenches its fluorescence emission. The PPy film ensures the protein is distanced from the gold and, at the same time, allows proteins to remain immobilized and retain their tertiary structure.

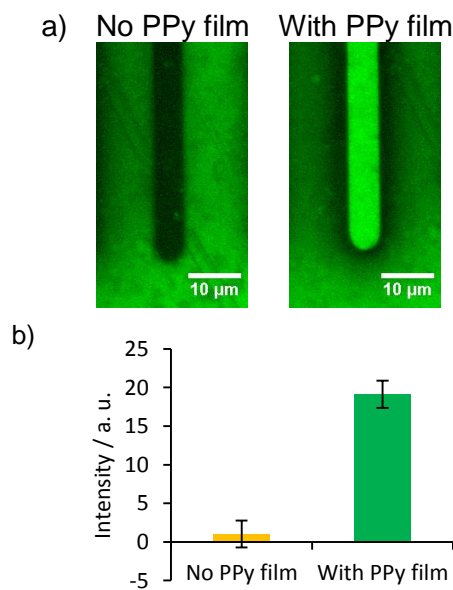


Figure 28. (a) GFP filter images of the electrodes functionalized while applying an electric field in the absence and in the presence of the PPy film. (b) Increase in fluorescence intensity for the electrodes in the absence and presence of the PPy film.

It should also be noted that the background signal on the SiO₂ surface is very inconsistent as seen from the comparison between figures 27 and 28. On the images shown in this thesis, this signal depends mostly on the electrode array used, as some of the arrays show nearly no background signal while others show a very high signal. The reason behind this was identified by a post-doc in the group, Eduardo Della Pia, who was working with the same kind of arrays. The arrays with a high background signal showed some traces of the resist film from the fabrication process and it is this film that promoted the protein adsorption to the background.

Regarding the stability of the immobilized protein, samples imaged one week after immobilization have shown no change in the fluorescence emission (data not shown).

As seen from figure 29, when applying 0 mV on the working electrode during the functionalization of the PPy film, the fluorescence intensity is approximately half than when applying 600 mV. This difference is slightly accentuated when applying -300 mV during the functionalization of the PPy film as the intensity of the electrode functionalized while applying 600 mV is 2.5-fold higher than the electrode functionalized while applying -300 mV. H₆-EGFP has a theoretical pI of 6.13, so at pH 7.4, it is negatively charged. Therefore, it makes sense that when applying a positive potential we can direct the protein onto the working electrode, but, when applying a negative potential, electrostatic repulsion should prevent the protein from binding. The repulsion effect should grow, as we decrease the potential applied.

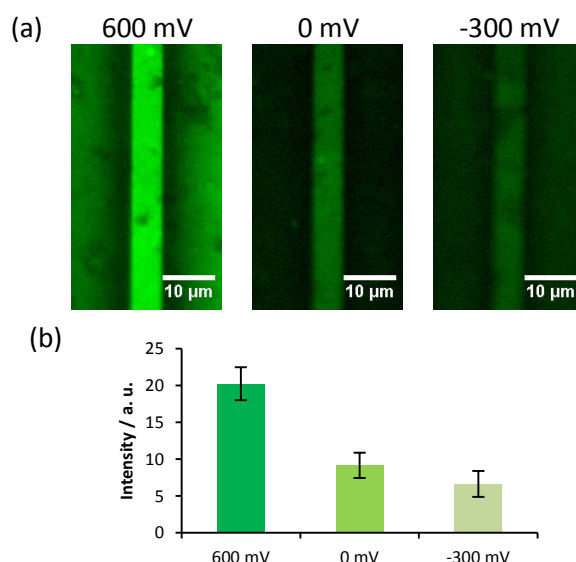


Figure 29. (a) GFP filter images of electrodes functionalized while applying different potentials. (b) Increase in fluorescence intensity of the shown electrodes.

SFH₁₀-647 was also used to functionalize the electrodes. In order to optimize conditions 600mV and 800 mV (any higher voltages could result in damage to the PPy

film) were applied to the PPy covered electrodes for 120 s. When applying 600 mV on the electrode no change in the fluorescence intensity was detected (data not shown). Then, to test the duration of the potential, 800 mV were applied on the electrode for 120 s and 600 s, each one showing a small increase in emission but very little difference among them (figure 30). On the other hand, the control kept in an open circuit, showed no increase in the fluorescence intensity. The results demonstrate that when applying 800 mV on the electrode, SFH₁₀-647 is directed onto the PPy film.

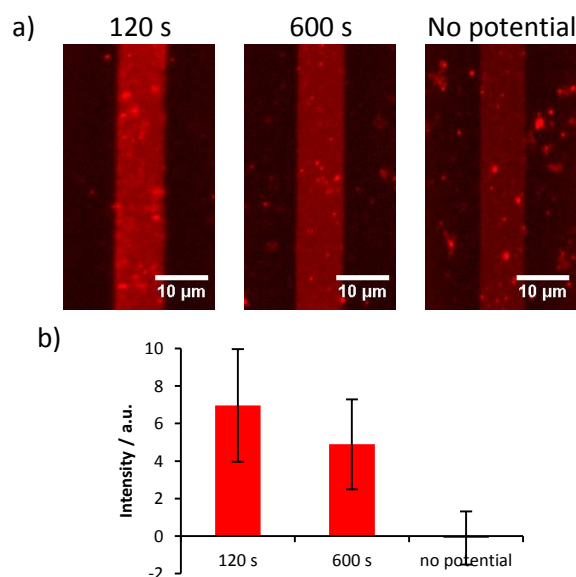


Figure 30. (a) Cy5 images of 3 different electrodes functionalized with SFH₁₀-647. On the electrode on the left, 800 mV were applied for 120 s. On the electrode in the middle, 800 mV were applied for 600s. The electrode on the right was kept in an open circuit. (b) Increase in fluorescence intensity for the conditions described in (a).

In order to investigate the influence of the his-tag on protein binding. Cleaved SFH₁₀-647 was immobilized on a PPy film while applying 800 mV for 120 s. Figure 31 shows the comparison between the immobilization of the full SFH₁₀-647 and the cleaved version of the protein. The electrode functionalized with cleaved SFH₁₀-647 shows half the intensity of the electrode functionalized with SFH₁₀-647. Still, the intensity of the electrode functionalized with cleaved SFH₁₀-647 is closer to the intensity of the electrode functionalized with SFH₁₀-647 while applying 800 mV than when the PPy film was functionalized in open-circuit (figure 30). The difference between the immobilization of the cleaved SFH₁₀-647 and SFH₁₀-647 can also be explained by the higher amount of protein aggregates in solution. The aggregates deposit on the surface instead of being directed onto the working electrode.

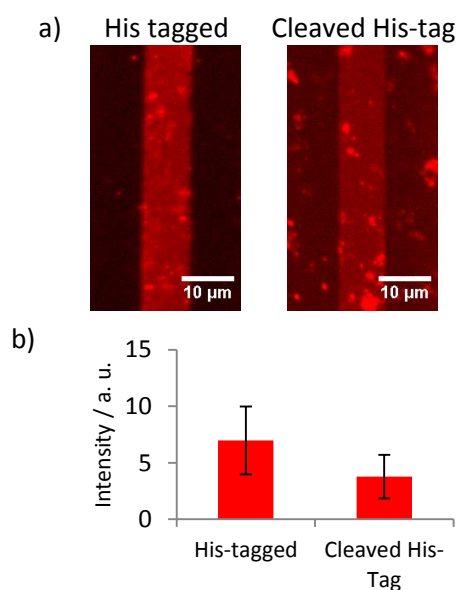


Figure 31. (a) Cy5 images of different electrodes functionalized with SFH10-647 and the same protein with the his-tag cleaved. (b) Increase in fluorescence intensity for the electrodes functionalized with SFH₁₀-647 and the cleaved version of the protein.

The previous experiments aimed at setting conditions to direct both H₆-EGFP and SFH₁₀-647 onto the electrodes. Using the set conditions, H₆-EGFP and SFH₁₀-647 were sequentially immobilized on two different electrodes. After functionalization of the second electrode there is only a very small increase in the previously functionalized electrode. Furthermore, the activated electrode shows high fluorescence intensity. The fact that the increase is higher than in the previous experiments can be related to the absence of aggregates from the protein sample used in this case.

In order to demonstrate the generation of PPy followed by its functionalization can be used to immobilize different proteins on different electrodes of an array, two electrodes were functionalized with H₆-EGFP and SFH₁₀-647 (figure 32). After generation of a PPy film, H₆-EGFP was immobilized while applying 600 mV for 120s on the PPy covered electrode, followed by generation of a second PPy film on an adjacent electrode and its functionalization while applying 800 mV for 120s. The results show that both proteins have been successfully immobilized on the electrode array.

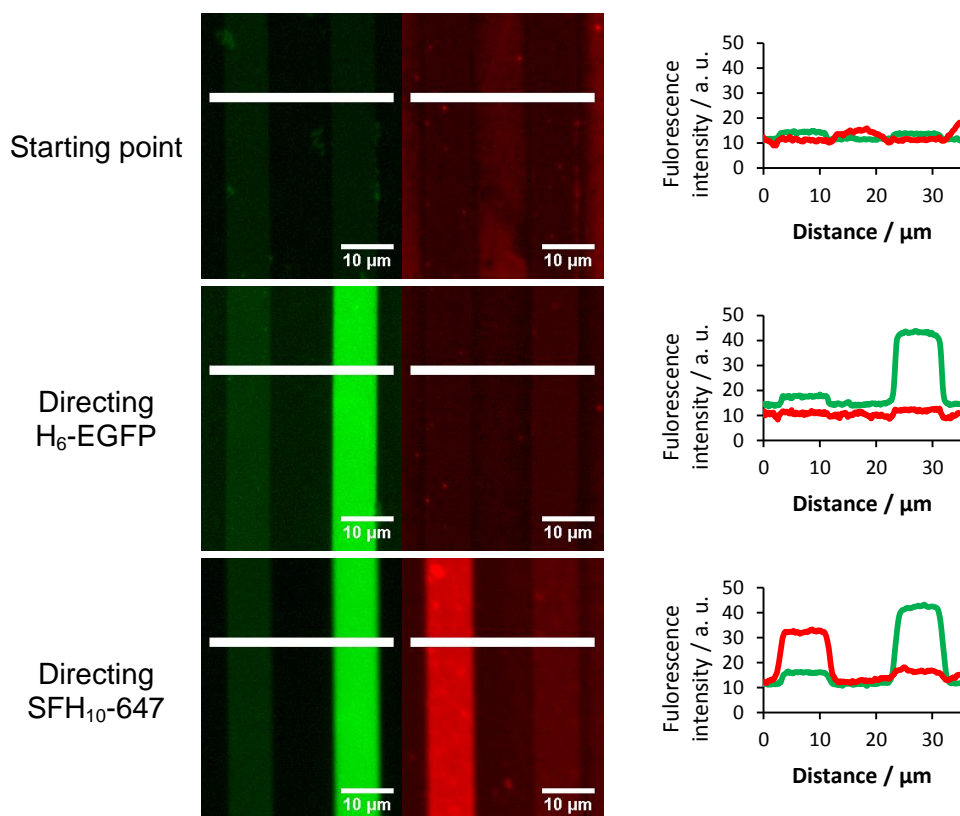


Figure 32. Sequential immobilization of H₆-EGFP and SFH₁₀-647 on two different electrodes. On the left, it is shown the GFP and Cy5 filter images, respectively, throughout the different immobilizations. On the right, line scans taken from the GFP (—) and Cy5 filter (—) images on the left

In order to demonstrate that the use of electrical fields can be used for multiplexing different proteins on different electrodes already covered with PPy without requiring the generation of a new PPy film prior to the immobilization of each protein, a PPy film was generated on three different electrodes and then protein was directed onto each one sequentially. Figure 33 shows the different steps of this functionalization strategy. On the first immobilization step, 600 mV were applied on the first electrode (from left to right) for 30 s. On the second immobilization step, 600 mV were applied on the third electrode (from left to right) for 60 s. On the final immobilization step, 600 mV were applied on the fourth electrode (from left to right) for 60 s. These results also suggest the longer duration of the electric fields applied to the electrodes, does not influence protein binding.

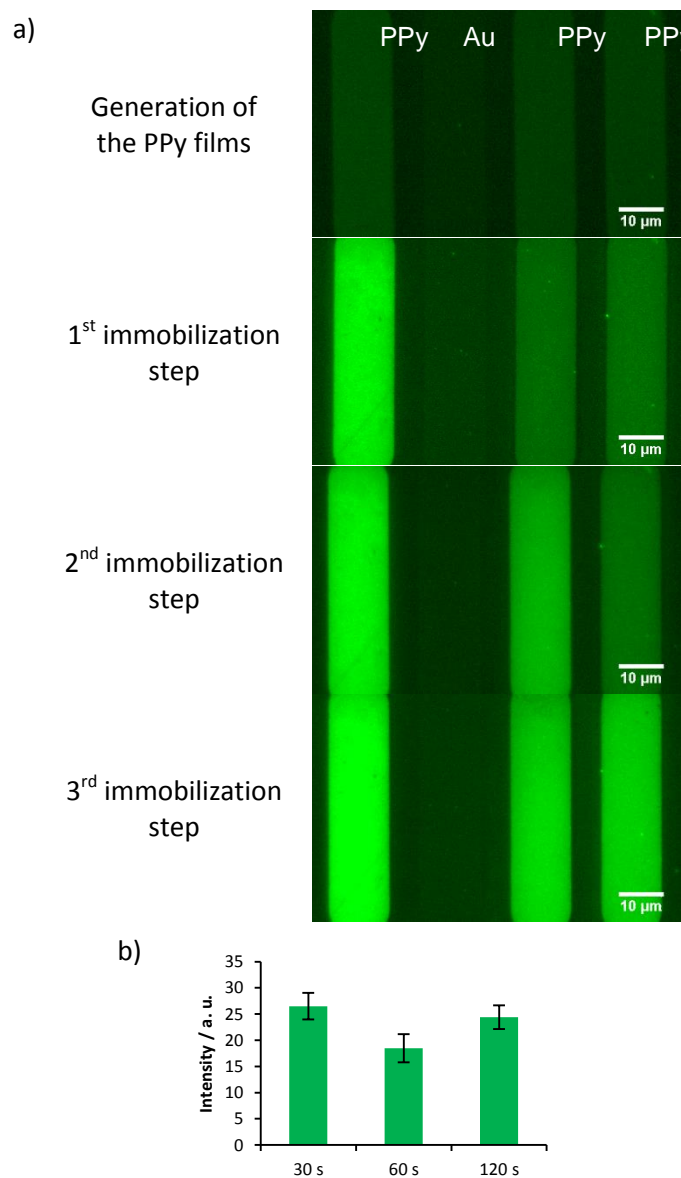


Figure 33. (a) GFP filter images of the sequential functionalization of 3 different electrodes with H₆-EGFP. For the 1st immobilization step, 600 mV were applied to the first electrode (from left to right) for 30 s. For the 2nd immobilization step, 600 mV were applied to the third electrode (from left to right) for 60 s. For the 3rd immobilization step, 600 mV were applied to the fourth electrode (from left to right) for 120 s (b) Increase in fluorescence intensity in relation to the non-functionalized PPy films when applying a potential on the shown electrodes for different periods of time.

The functionalization of PPy films was extended to nanometer electrodes. Figure 34 shows 300 nm-wide electrodes designed in a spiral and figure 35 shows an electrode with indentations which are as low as 80 nm wide. The electrodes were functionalized with H₆-EGFP while applying 600 mV for 30 s on the PPy covered electrode. The resolution of the microscope is not high enough to visualize such small structures, however an homogeneous coverage of all the electrodes can be observed.

The results indicate it is possible to use nano-sized electrodes in order to fabricate protein nanoarrays.

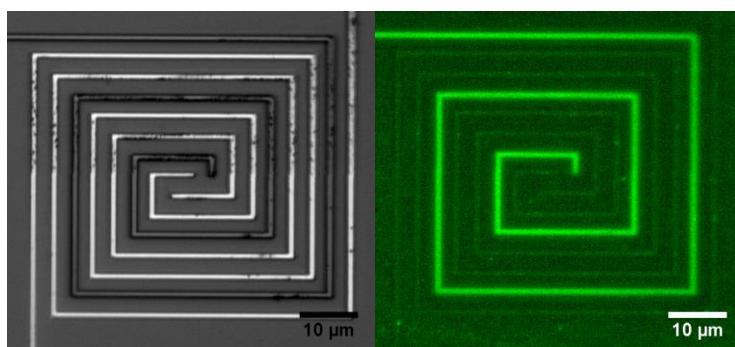


Figure 34. DIC and GFP filter images of two non-functionalized electrodes and one functionalized with H₆-EGFP designed in a spiral. The width of each electrode is 300 nm.

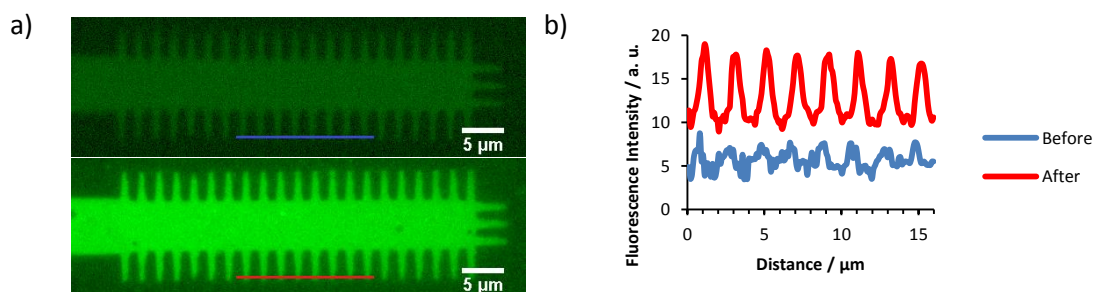


Figure 35. GFP filter images of an electrode before (on top) and after (on bottom) functionalization. The width of the indentations decreases with the distance to the center of the electrode and reaches ~80 nm at the tip. (b) line scans from the images shown.

4.4. Conclusion

In this chapter I report sequential electropolymerization of PPy films as a route to achieve protein multiplexing. This approach allows one to generate a polymer film with the desired pattern, being limited only by the current electrode fabrication techniques. As shown, the generation and functionalization of PPy films can be done in a nanoscale regime, making this a promising tool in the development of protein nanoarrays.

The functionalization strategy reported in this chapter uses electric fields to enhance protein physisorption. By using a positive potential it was possible to enhance the adsorption of negatively charged proteins onto the surface of previously generated PPy films. This approach is quite soft as no changes in pH are required and, in principle, conditions can be optimized for a variety of proteins.

Two his-tagged proteins and one protein with the his tag cleaved were successfully immobilized on PPy covered electrodes. As the his-tag does not influence the binding of the proteins, it should be possible to use this strategy as a way to increase the amount of protein adsorbed without chemically modifying the protein or using fusion proteins. This may prove especially useful in the immobilization of antibodies and the development of immunoarrays.

Furthermore the use of electrically contacted surfaces is, by itself, an exciting strategy towards label-free biosensing as any change to these surfaces can be translated into an electrical signal. The incorporation of electrode arrays in microfluidic devices may not only enhance their potential as a biosensor but may also help optimize conditions used to generate the polymer films (especially by having a higher control over the washing steps) and functionalization conditions.

Chapter 5.

Summary and Perspectives

The work presented in this thesis focus on the immobilization of proteins on surfaces. This topic has attracted a lot of attention, especially with the development of bionanotechnology. This thesis reported the expression of two model proteins, H₆-EGFP and SFH₁₀ and the use of two different approaches to immobilize these proteins onto solid supports. The first approach used relied on the interaction of an his-tag in the aminoacidic chain of the protein and the Ni-NTA motifs on the surface of polystyrene microparticles. This reversible interaction allows proteins to be attached to the surface with a defined orientation, which may contribute towards the protein retaining its activity.

The binding of H₆-EGFP onto Ni-NTA polystyrene microparticles was investigated using fluorescence spectroscopy and fluorescence microscopy. While fluorescence spectroscopy accounts for the concentration of fluorophore in solution, and therefore depends on the surface area available, fluorescence microscopy allows the monitoring of single particles. The functionalization of NiNTA-PPsMPs in solution with H₆-EGFP, followed by analysis by fluorescence spectroscopy, has shown the amount of protein to be too inconsistent. However this might be a result of small changes in all the parameters that need to be considered.

The binding of of H₆-EGFP onto immobilized NiNTA-PPsMPs was investigated using fluorescence microscopy. As it is possible to monitor particles individually it might be possible to optimize the analysis of the system to track different signals, including the size, aspect ratio. One of the main problems faced in this work was the background signal, as a high decrease in the background intensity originates a false intensity signal from the particles. Further optimization of the properties of the intermediate layer between the NiNTA-PPsMPs and the glass surface may allow avoiding this problem.

Functionalization of NiNTA-PPsMPs in solution followed by their immobilization on a glass surface may prove to be an easy, fast and cheap way to produce protein microarrays. Miniaturization of the particles may also play an important role in the development of such system. The use of particles to create protein spots, in principle, is not limited to microparticles. By using nanoparticles, one may be able to reduce the area which needs to be covered by proteins and, at the same time, increase the number of proteins which can be immobilized on the same array.

The second approach reported in this thesis used the sequential electrogeneration and functionalization of PPy films to achieve protein multiplexing. Furthermore, it is also shown that the use of an electric field enhances the amount of protein adsorbed onto the polypyrrole film. This strategy has shown promising results towards the high-throughput, highly parallel fabrication of protein micro- and nanoarrays. By functionalizing the polypyrrole films immediately after their generation, we can select

the area to functionalize without preventing any further functionalization of the remaining electrodes. This strategy also presents some disadvantages. Each time a new film is polymerized, the whole surface is exposed to the monomeric pyrrole solution. Therefore, it is important to control the composition of this solution to prevent previously immobilized proteins from getting denatured.

The use of electric fields in order to enhance protein adsorption may prove to be an invaluable strategy to help the fabrication of these devices. The fact that protein adsorption is enhanced by applying an electric field is, by itself, important as it allows faster and cheaper procedures. Additionally, the use of electric fields not only to direct proteins to the surface but also to repel the proteins might be used to achieve protein multiplexing while avoiding the need for the proteins to be exposed to the polymerization solution. Still, before scaling up this procedure, it is important to assess the accessibility of the immobilized proteins.

This thesis has shown protein immobilization to the PPy film by physisorption, but these strategies might also be applicable to doped PPy films or films from pyrrole derivatives containing biotin, NTA or other motifs which can be used to selectively attach proteins. This would allow proteins to be immobilized with a specific orientation improving the sensitivity of the system.

Finally, as this system relies on electrode arrays, one possible application would be for label-free biosensing. The development in bioelectroanalytical techniques has opened the way towards this goal and the development of systems which can be integrated in electrical circuits may play an important role in bionanoanalytics or in bionanomedicine in the near future. By incorporating proteins into a conductive polymer film it should be possible to translate any changes to the protein, such as the binding of a target molecule, into an electrical signal and monitor the presence of the target molecule.

References

- [1] Gonzalez-Gonzalez, M., Jara-Acevedo, R., Matarraz, S., Jara-Acevedo, M., Paradinas, S., Sayagües, J. M., ... Fuentes, M. (2012). Nanotechniques in proteomics: protein microarrays and novel detection platforms. *European journal of pharmaceutical sciences : official journal of the European Federation for Pharmaceutical Sciences*, 45(4), 499–506;
- [2] Biswas, A., Bayer, I. S., Biris, A. S., Wang, T., Dervishi, E., & Faupel, F. (2012). Advances in top-down and bottom-up surface nanofabrication: techniques, applications & future prospects. *Advances in colloid and interface science*, 170(1-2), 2–27;
- [3] Ramachandran, N., Srivastava, S., & LaBaer, J. (2008). Applications of protein microarrays for biomarker discovery. *Proteomics Clin. Appl.*, 2 , 10-11, 1444–1459;
- [4] Jiang, W., Huang, R., Duan, C., Fu, L., Xi, Y., Yang, Y., Huang, R.-P. (2013). Identification of five serum protein markers for detection of ovarian cancer by antibody arrays. *PloS one*, 8, 10, e76795
- [5] Sereni, M. I., Pierobon, M., Angioli, R., Iii, E. F. P., & Frederick, M. J. (2013). Target Identification and Validation in Drug Discovery. In J. Moll & R. Colombo (Eds.), *Target Identification and Validation in Drug Discovery* (Vol. 986, pp. 187–214). Totowa, NJ: Humana Press;
- [6] Price, J. V, Tangsombatvisit, S., Xu, G., Yu, J., Levy, D., Baechler, E. C., ... Liu, C. L. (2012). On silico peptide microarrays for high-resolution mapping of antibody epitopes and diverse protein-protein interactions. *Nature medicine*, 18, 9, 1434–40;
- [7] Jonkheijm, P., Weinrich, D., Schröder, H., Niemeyer, C. M., & Waldmann, H. (2008). Chemical strategies for generating protein biochips. *Angewandte Chemie (International ed. in English)*, 47, 50, 9618–47;
- [8] De Mol, N. J. (2012). Surface Plasmon Resonance for Proteomics. In E. D. Zanders (Ed.), *Chemical Genomics and Proteomics* (Vol. 800, pp. 33–53). Totowa, NJ: Humana Press;
- [9] Ongaro, M., & Ugo, P. (2013). Bioelectroanalysis with nanoelectrode ensembles and arrays. *Analytical and bioanalytical chemistry*, 405, 11, 3715–29;
- [10] Tang, Q., Shi, S.-Q., & Zhou, L. (2004). Nanofabrication with Atomic Force Microscopy. *Journal of Nanoscience and Nanotechnology*, 4, 8, 948–963;
- [11] Gates, B. D., Xu, Q., Stewart, M., Ryan, D., Willson, C. G., & Whitesides, G. M. (2005). New approaches to nanofabrication: molding, printing, and other techniques. *Chemical reviews*, 105, 4, 1171–96;
- [12] Manfrinato, V. R., Zhang, L., Su, D., Duan, H., Hobbs, R. G., Stach, E. a, & Berggren, K. K. (2013). Resolution limits of electron-beam lithography toward the atomic scale. *Nano letters*, 13, 4, 1555–8;
- [13] Piner, R. D., Zhu, J., Xu, F., Hong, S., & Mirkin, C. A. (1999). “Dip-Pen” Nanolithography. *Science*, 283, 661–663;

- [14] Salaita, K., Wang, Y., Fragala, J., Vega, R. a, Liu, C., & Mirkin, C. a. (2006). Massively parallel dip-pen nanolithography with 55 000-pen two-dimensional arrays. *Angewandte Chemie (International ed. in English)*, 45, 43, 7220–3;
- [15] Zheng, Z., Daniel, W. L., Giam, L. R., Huo, F., Senesi, A. J., Zheng, G., & Mirkin, C. a. (2009). Multiplexed protein arrays enabled by polymer pen lithography: addressing the inking challenge. *Angewandte Chemie (International ed. in English)*, 48, 41, 7626–9;
- [16] Rich, R. L., & Myszka, D. G. (2000). Advances in surface plasmon resonance biosensor analysis. *Current opinion in biotechnology*, 11, 1, 54–61;
- [17] Abbas, A., Linman, M. J., & Cheng, Q. (2011). New trends in instrumental design for surface plasmon resonance-based biosensors. *Biosensors & bioelectronics*, 26, 5, 1815–24;
- [18] Rusmini, F., Zhong, Z., & Feijen, J. (2007). Protein immobilization strategies for protein biochips. *Biomacromolecules*, 8, 6, 1775–89;;
- [19] Turková, J. (1999). Oriented immobilization of biologically active proteins as a tool for revealing protein interactions and function. *Journal of chromatography. B*, 722 ,1-2, 11–31;
- [20] Smith, C. L., Milea, J. S., & Nguyen, G. (2006). Immobilization of Nucleic Acids Using Biotin-Strept (avidin) Systems. *Top Curr Chem*, 261, 63–90;
- [21] Kruppa, M., & König, B. (2006). Reversible coordinative bonds in molecular recognition. *Chemical reviews*, 106, 9, 3520–60;
- [22] Gautier, A., Juillerat, A., Heinis, C., Corrêa, I. R., Kindermann, M., Beaufils, F., & Johnsson, K. (2008). An engineered protein tag for multiprotein labeling in living cells. *Chemistry & biology*, 15, 2, 128–36;
- [23] Shimonura, O. (2008) Discovery of Green Fluorescent Protein, GFP. Nobel Lecture;
- [24] Shimonura, O., Johnson, F. H., & Saiga, Y. (1962). Extraction , Purification and Properties of Aequorin , a Bioluminescent Protein from the Luminous. *J Cell Comp Physiol.*, 59, 223–239;
- [25] Chalfie, M. (2008) GFP: Lighting Up Life. Nobel Lecture;
- [26] Chalfie, M., Tu, Y., Euskirchen, G., Ward, W. W., & Prasher, D. C. (1994). Green fluorescent protein as a marker gene expression. *Science*, 263, 802–805;
- [27] Tsien, R.Y. (2008) Constructing and Exploiting the Fluorescent Protein Paintbox. Nobel Lecture;
- [28] Heim, R., Cubitt, A., & Tsien, R. Y. (1995). Improved Green Fluorescence. *Nature*, 373, 663–664;
- [29] Cormack, B. P., Valdivia, R. H., & Falkow, S. (1996). FACS-optimized mutants of the green fluorescent protein (GFP). *Gene*, 173, 1 Spec No, 33–8;

- [30] Ormö, M., Cubitt, a B., Kallio, K., Gross, L. a, Tsien, R. Y., & Remington, S. J. (1996). Crystal structure of the *Aequorea victoria* green fluorescent protein. *Science*, 273, 1392–1395;
- [31] Cotlet, M., Hofkens, J., Maus, M., Gensch, T., Van der Auweraer, M., Michiels, J., De Schryver, F. C. (2001). Excited-State Dynamics in the Enhanced Green Fluorescent Protein Mutant Probed by Picosecond Time-Resolved Single Photon Counting Spectroscopy. *The Journal of Physical Chemistry B*, 105, 21, 4999–5006;
- [32] Keppler, A., Gendreizig, S., Gronemeyer, T., Pick, H., Vogel, H., & Johnsson, K. (2003). A general method for the covalent labeling of fusion proteins with small molecules in vivo. *Nature biotechnology*, 21, 1, 86–9;
- [33] Keppler, A., Pick, H., Arrivoli, C., Vogel, H., & Johnsson, K. (2004). Labeling of fusion proteins with synthetic fluorophores in live cells. *Proceedings of the National Academy of Sciences of the United States of America*, 101, 27, 9955–9;
- [34] Liu, Y.-C. C., Rieben, N., Iversen, L., Sørensen, B. S., Park, J., Nygård, J., & Martinez, K. L. (2010). Specific and reversible immobilization of histidine-tagged proteins on functionalized silicon nanowires. *Nanotechnology*, 21, 24, 245105;
- [35] Barbee, K. D., Hsiao, A. P., Roller, E. E., & Huang, X. (2010). Multiplexed protein detection using antibody-conjugated microbead arrays in a microfabricated electrophoretic device. *Lab on a chip*, 10, 22, 3084–93;
- [36] Lauer, S. A., & Nolan, J. P. (2002). Development and Characterization of Ni-NTA-Bearing Microspheres, 48, 136–145;
- [37] Jones, C.J. *d- and f- Block Chemistry*. Wiley-RSC. 2002. 1st edition;
- [38] Atkins, P., Overton, T., Rourke, J., Weller., Armstrong F. *Shriver and Atkins' Inorganic Chemistry*. OUP Oxford. 2009. 5th edition;
- [39] Langmuir, I. (1916). The Constitution and Fundamental Properties of Solids and Liquids. Part I. Solids. *J Am Chem Soc*, 38, 2221–2295;
- [40] Masel, R.I. *Principles of Adsorption and Reaction on Solid Surfaces*. John Wiley & Sons, Inc. 1996. New York;
- [41] Clark, L. C., Lyons, C. (1963) Electrode Systems for Continuous Monitoring in Cardiovascular Surgery. *Annals of the New York Academy of Sciences*, 102, 29, 1963;
- [42] Cosnier, S. (2003). Biosensors based on electropolymerized films: new trends. *Analytical and bioanalytical chemistry*, 377,3, 507–20;
- [43] Cosnier S, Gondran C, Watelet JC (2001) A Polypyrrole-Bienzyme Electrode (Salicylate Hydroxylase-Polyphenol Oxidase) for the Interference-Free Determination of Salicylate. *Electroanalysis*. 13, 906–910;
- [44] Serradilla Razola S, Lopez Ruiz B, Mora Diez N, Mark Jr HB, Kauffmann J-M (2002) Hydrogen peroxide sensitive amperometric biosensor based on horseradish peroxidase entrapped in a polypyrrole electrode. *Biosens Bioelectron*. 17, 921–928;

- [45] Haddour, N., Cosnier, S., & Gondran, C. (2005). Electrogeneration of a poly(pyrrole)-NTA chelator film for a reversible oriented immobilization of histidine-tagged proteins. *Journal of the American Chemical Society*, 127, 16, 5752–3;
- [46] Baur, J., Holzinger, M., Gondran, C., & Cosnier, S. (2010). Immobilization of biotinylated biomolecules onto electropolymerized poly(pyrrole-nitrilotriacetic acid)-Cu²⁺ film. *Electrochemistry Communications*, 12, 10, 1287–1290;
- [47] Darmanin, T., Bellanger, H., Guittard, F., Lisboa, P., Zurn, M., Colpo, P., Rossi, F. (2012). Structured biotinylated poly(3,4-ethylenedioxyppyrole) electrodes for biochemical applications. *RSC Advances*, 2, 3, 1033;
- [48] Stern, E., Jay, S., Bertram, J., Boese, B., Kretzschmar, I., Turner-Evans, D., Reed, M. a. (2006). Electropolymerization on microelectrodes: functionalization technique for selective protein and DNA conjugation. *Analytical chemistry*, 78, 18, 6340–6;
- [49] Reuss, F.F. (1809). *Mem. Soc. Imperiale Naturalistes de Moscow*. 2: 327;
- [50] Tiselius, Arne (1937). "A new apparatus for electrophoretic analysis of colloidal mixtures". *Transactions of the Faraday Society* 33: 524–531;
- [51] Scott, R.P.W. Physical Chemistry Resources. Book 3. Electrophoresis;
- [52] Wong, I. Y., & Melosh, N. a. (2009). Directed hybridization and melting of DNA linkers using counterion-screened electric fields. *Nano letters*, 9(10), 3521–6.

Annexes

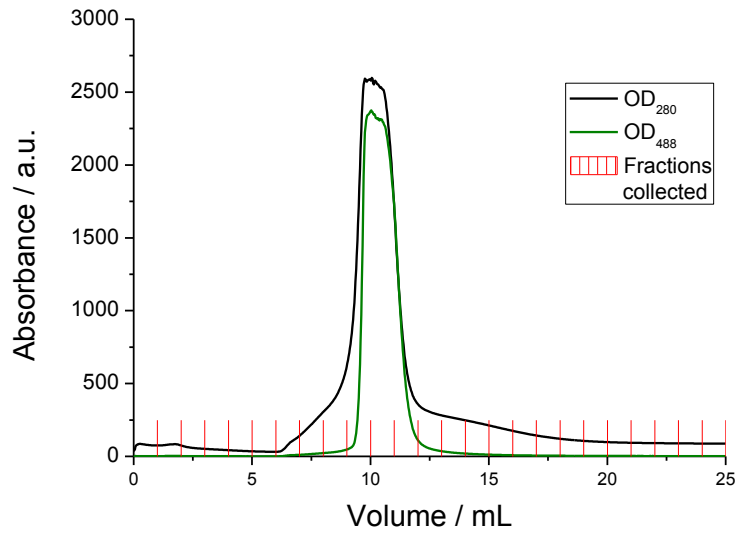
Aminoacid sequence of H₆-EGFP

MGSSHHHHHH SSGLVPRGSH MVSKGEELFT GVPILVELD GDVNGHKFSV
[50] SGEGEGDATY GKLTLKFICT TGKLPVPWPT LVTTLTYG VQ CFSRYPDHMK
[100] QHDFFKSAMP EGYVQERTIF FKDDGNYKTR AEVKFEGDTL VNRIELKGID
[150] FKEDGNILGH KLEYNYNSHN VYIMADKQKN GIKVNFKIRH NIEDGSVQLA
[200] DHYQQNTPIG DGPVLLPDNH YLSTQSALSK DPNEKRDH MV LLEFVTAAGI
[250] TLGMDELYK

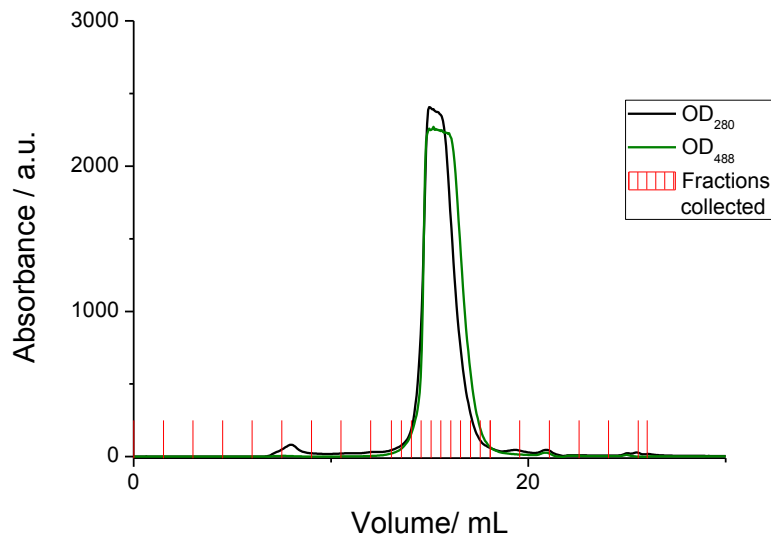
Aminoacid sequence of SFH₁₀

MDKDCEMKRT TLDSP LGKLE LSGCEQGLHE IKLLGKG TSA ADAVEVPAPA
[50] AVLGGPEPLM QATAWLNAYF HQPEAIEEFP VPALHHPVFQ QESFTRQVLW
[100] KLLKVVKFGE VISYQQLAAL AGNPAATAAV KTALSGNPVP ILIPCHRVVS
[150] SSGAVGGYEG GLAVKEWLLA HEGHRLGKPG LGPAGIGAPG SDYKDDDDKE
[200] FHHHHHHHHH H

Chromatograms from the 2nd time H₆-EGFP was expressed and purified

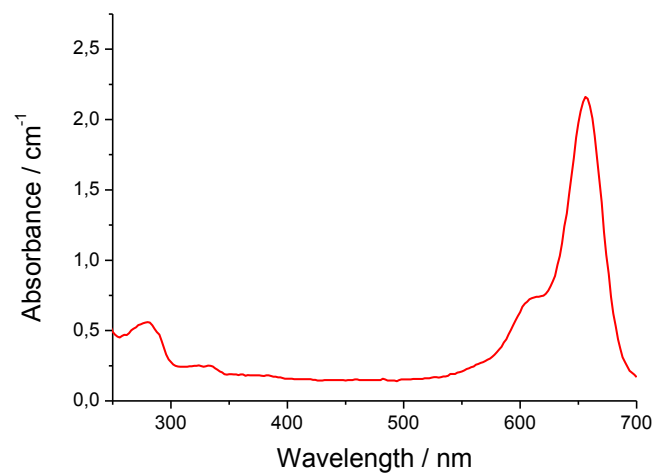


Supplementary Figure 1. Chromatogram from the IMAC of H₆-EGFP. Fractions 10,11 and 12 were used for further purification.



Supplementary Figure 2. Chromatogram from the SEC of H₆-EGFP. Fractions 12 to14 were used for further experiments.

Absorbance spectrum of SFH₁₀-647 used for the determination of the DOL of the labeled protein sample.



Supplementary Figure 3. Absorbance spectrum of SFH₁₀-647. The absorbance was corrected to a pathlength of 1 cm.